J. Membrane Biol. 73, 69–89 (1983)

The Journal of
Membrane Biology

Cell-to-Cell Channels with Two Independently Regulated Gates in Series: Analysis of Junctional Conductance Modulation by Membrane Potential, Calcium, and pH

Ana Lia Obaid*, Sidney J. Socolar, and Birgit Rose
Department of Physiology and Biophysics, University of Miami School of Medicine, Miami, Florida 33101

Summary. We study cell-to-cell channels, in cell pairs isolated from *Chironomus* salivary gland, by investigating the dependence of junctional conductance (g_j) on membrane potentials (E_1, E_2), on Ca^{2+}, and on H^+, and we explore the interrelations among these dependencies; we use two separate voltage clamps to set the membrane potentials and to measure g_j. We find g_j to depend on membrane potentials whether or not a transjunctional potential is present. The pattern of g_j dependence on membrane potentials suggests that each channel has two closure mechanisms (gates) in series. These gates pertain, respectively, to the two cell faces of the junction. By treating the steady-state g_j as the resultant of two simultaneous but independent voltage-sensitive open/closed equilibria, one within each population of gates (i.e., one on either face of the junction), we develop a model to account for the steady-state g_j *vs.* E relationship. Elevation of cytosolic Ca^{2+} or H^+ at fixed E lowers g_j, but at moderate concentrations of these ions this effect can be completely reversed by clamping to more negative E. Overall, the effect of a change in pCa_i or pH_i takes the form of a parallel shift of the g_j *vs.* E curve along the E axis, without change in slope. We conclude (1) that the patency of a cell-to-cell channel is determined by the states of patency of its two gates; (2) that the patency of the gates depends on membrane potentials (not on transjunctional potential), on pCa_i, and on pH_i; (3) that pCa_i and pH_i determine the position of the g_j *vs.* E curve on the E axis; and (4) that neither Ca^{2+} nor H^+ at moderate concentrations alters the voltage sensitivity of g_j.

Key Words cell-to-cell channels · junctional conductance · cell junctional permeability · intercellular communication · voltage-dependent conductance · membrane potential · calcium · pH

Introduction

In many tissues, cells are joined to each other by conductive cell-to-cell channels (Loewenstein, 1981). These channels can close reversibly; the conductance of a cell junction thus depends on the number of open channels. Apparently, the closure mechanism can be activated from either cell partner of a junction by elevation of cytoplasmic Ca^{2+} (Loewenstein, Nakas & Socolar, 1967; Oliveira-Castro & Loewenstein, 1971; Rose & Loewenstein, 1976; Spray et al., 1982*a, b*; but *see also* Johnston & Ramon, 1981), or of cytoplasmic H^+ (Rose & Rick, 1978; Spray et al., 1982*a, b*; but *see also* Johnston & Ramon, 1981), and by lowering membrane potential (Socolar & Politoff, 1971).

We currently picture each cell-to-cell channel as arising from the union of two identical *hemi*-channels, one from each cell partner of a junction (Loewenstein, 1981). The indication that channel patency (openness) can be modified from either cytoplasmic face of a junction raises the question, whether each *hemi*channel contributes a separate gate capable of shutting the *channel* – a gate that is controlled entirely by that cell to which the hemichannel pertains. We endeavor to answer this question by investigating the dependence of junctional conductance on membrane potential. We propose a thermodynamic model, based on a population of channels, each with two independent voltage-sensitive gates in series, to account for the relationship between membrane potential and steady-state cell-to-cell conductance. In addition, we consider whether the effects of membrane potential on the one hand and of Ca^{2+} and H^+ on the other are mediated by the same set of gates. We explore these points in cell pairs isolated from salivary glands of *Chironomus*.

Some of our results have already been reported in preliminary form (Obaid & Rose, 1981*a, b*).

Materials and Methods

Media

We used the following media: *"TC Medium"*: a 1:1 mixture of TC-199 (GIBCO medium 199, Hanks' salts) and Melnick's with L-glutamine and fetal calf serum added to yield a final concentration of 2 mM and 10%, respectively, and adjusted to

* *Present address:* Department of Physiology and Pharmacology, University of Pennsylvania School of Dental Medicine, Philadelphia, PA 19104.

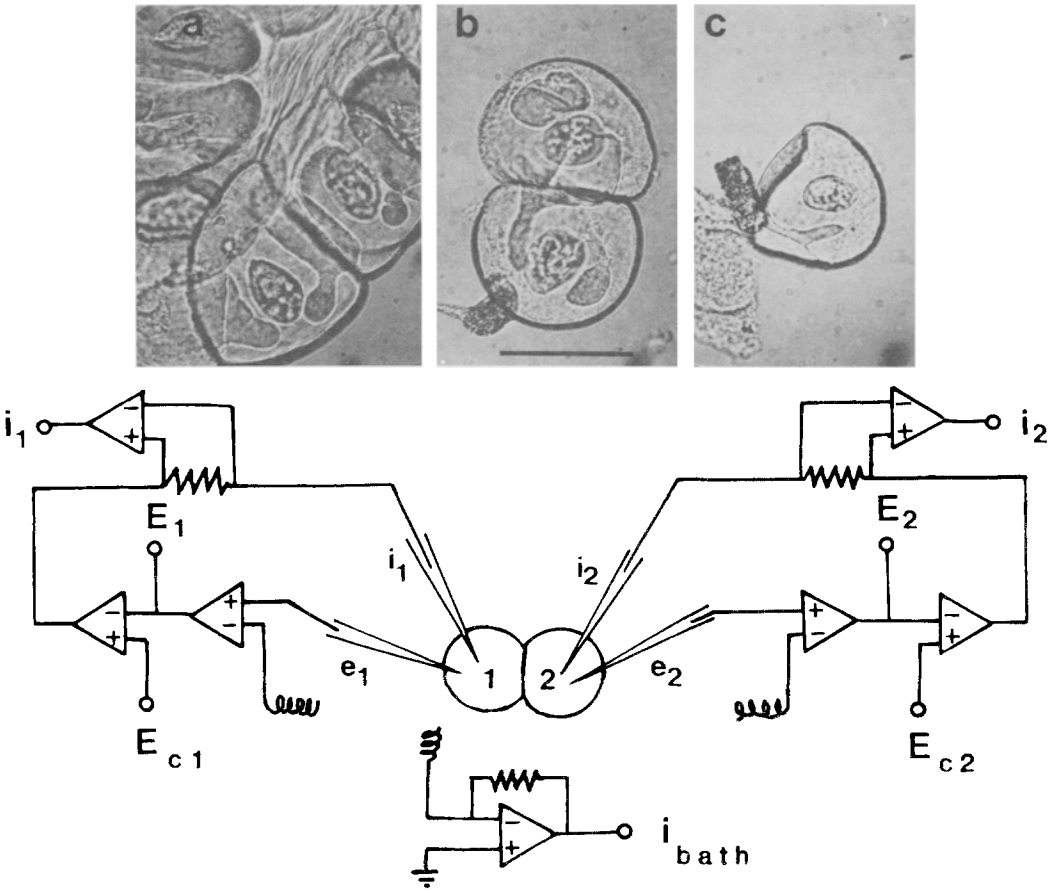

Fig. 1. *(Top):* Photomicrographs of (*a*) cells in an intact gland; (*b*) an enzymatically isolated cell pair, and (*c*) a single cell. Calibration, 100 μm for all pictures. *(Bottom):* Schematic of double voltage clamp for measurement of junctional conductance, g_j, between cells 1 and 2 of a pair. Each cell is impaled by a pair of microelectrodes, *e* and *i*, which is connected to an independent voltage-clamp circuit. The *e* electrodes measure cell potential with respect to the bath (coils represent Ag|AgCl electrodes connected to bath via 2.8 M KCl agar), which is held at virtual ground, and they are the references in their respective clamp circuits for comparison with the command voltage E_{c1} or E_{c2}, selected by the experimenter. The *i* electrodes also measure cell potential unless the instruments are in the "clamp" mode; then, current is injected through i_1 (i_2) whenever the cell potential E_1 (E_2) differs from the command potential, E_{c1} (E_{c2}). The total current flowing to the bath, $i_{bath}(=i_1+i_2)$, is recorded via an *I–V* converter connected to the bath. For measurements of junctional conductance g_j at a given potential *E*, both cells are initially clamped to that potential. After all traces show steady-state a small square voltage step ΔE_1 (3–5 mV, 1–2 sec) is superimposed on E_1. The steady-state current shift Δi_2 then generated by clamp circuit 2, to keep $E_2=E$, is equal and opposite to the current flowing through the junction, i_j. Then, junctional conductance $g_j=i_j/\Delta E_1$ where $i_j=-\Delta i_2$ and $E_j=E_1-E_2=\Delta E_1$. (*See Methods* for assessment of error in cases where the clamp gains were insufficient to maintain $E_2=E$ during ΔE_1, when we then calculate $g_j=\Delta i_2/(\Delta E_1-\Delta E_2)$.) All g_j values referred to in text were obtained by this protocol, and all conductances are steady-state chord conductances

pH 7.2 with NaOH. *"Melnick's"* (in mM): NaCl, 136.9; KCl, 5.36; $CaCl_2$, 1.76; $MgSO_4$, 0.46; $MgCl_2$, 0.49; Na_2HPO_4, 0.35; KH_2PO_4, 0.44; dextrose, 5.55; lactalbumin-hydrolysate, 10 g/liter; pH to 7.2 with NaOH. *"K-Melnick's"*: all Na in Melnick's was replaced with equimolar K. *"K_2SO_4-medium"* (mM): K_2SO_4, 100; $MgSO_4$, 2; EDTA, 1; TES, 5; glucose, 10; phenol red, 5 mg/liter; pH 7.3 with KOH. *"Enzyme medium"* for isolation of cell pairs and single cells: the following were added to "K_2SO_4-medium" (final concentration in mM): Na_2H_2ATP, 1; $CaCl_2$, 0.2; collagenase type II (Worthington Corp.), 100 units/ml; pH to 7.2 with KOH. *"Propionate medium"* (mM): Na-propionate, 40; Na_2fumarate, 28; Na_2succinate, 7; PIPES, 5; L-glutamine, 80; pH 6.8 with NaOH. All experiments were done at room temperature, 20–24 °C.

Isolation of Single Cells and Cell Pairs

About 20 to 40 salivary glands from *Chironomus thummi* larvae (9–11 days old) were obtained by dissection (Rose, 1971) in "Enzyme Medium" and placed in a dish. The glands were then gently stirred on a magnetic stirrer for 10–40 min. We inspected the dish at intervals, and, if cell doublets or triplets were found, they were transferred to another petri dish, containing "TC-medium," where they were reinspected after a few minutes. Often, one cell of the triplets or doublets would die in TC-medium, as evidenced by a swollen nucleus and granularity of the cytoplasm. An intact doublet, or if none was found, a triplet carefully stripped of its dead cell, was used for the experiment. The enzymatically isolated cells retained their char-

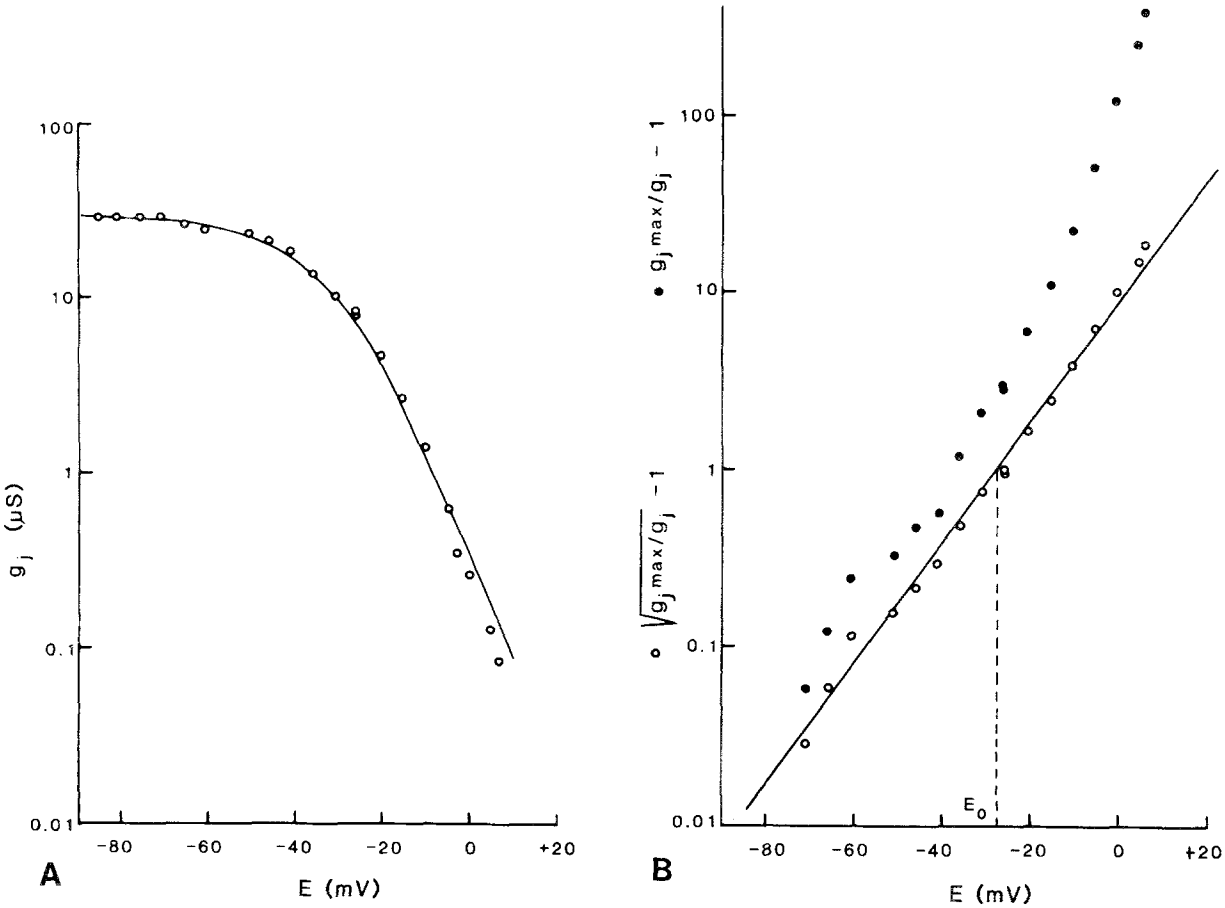

Fig. 2. Dependence of junctional conductance g_j on membrane potential E. *(A)*: Plot of g_j *vs.* E. Both cells of a cell pair were clamped to various but equal ($E_1 = E_2$) potentials E, and g_j was determined by application of a small voltage step ΔE_1 (3–5 mV, 1 sec) to cell 1; g_j was calculated (*see Methods*) as $-\Delta i_2/(\Delta E_1 - \Delta E_2)$. The protocol here was to move E in staircase fashion from the resting potential to more negative, then to more positive, and again to more negative potentials. Data (open circles) are the steady-state g_j measurements. *(B)*: Graphic representation of the analysis of the experimental data from *A* according to Eq. (5) (open circles) and Eq. (6) (filled circles) of the text. In both cases, the ordinate values were calculated with $g_j\,\mathrm{max} = 30$ μS. This gave a correlation coefficient $r = 0.996$ for the fit of the data to the line predicted by Eq. (5). The parameters obtained from this analysis are $A(\mathrm{slope}/2.3) = 0.077\ \mathrm{mV}^{-1}$; $E_0 = -27$ mV (E value at which the ordinate = 1), $z = ART/F = 2.0$. Using these parameters, we calculate $g_j(E) = 30/\{1 + \exp[0.077(E+27)]\}^2$ (μS) according to Eq. (4). The solid line drawn in *A* represents the g_j *vs.* E relationship thus calculated. The filled circles, which plot the data according to Eq. (6), do not fit a straight line, a fit that would be expected if g_j were the function of a single, and not of a compound, voltage-dependent probability (*see* Discussion)

acteristic complex shape, even as single cells (Fig. 1, top). They were viable in TC-medium for many hours, as judged by resting potential, input resistance and, in the case of cell pairs, junctional conductance.

Measurement of Junctional Conductance

To measure junctional conductance, g_j, between a pair of cells, we used a double voltage clamp system (Fig. 1, bottom). Each cell was impaled by a pair of microelectrodes *e* and *i* (Ultratip glass from Frederick Haer, Inc., filled with 0.5 M K_2SO_4), which was connected to its corresponding clamp circuit 1 or 2. The *e* electrodes measured the cells' potential with respect to the bath, which was held at virtual ground. The *i* electrodes also measured cell potentials, unless the instruments were in the "clamp" mode; then they passed currents (i_1, i_2) between the cell interior and the bath whenever the command voltage (E_{c1}, E_{c2}) deviated from the corresponding cell's potential (E_1, E_2). For measurement of g_j at any given potential E, both cells were initially clamped to that potential. After the clamp currents had reached steady state, a small square test pulse of voltage, ΔE_1 (3–5 mV, 1–2 sec) was superimposed on E_1. From the steady-state current shift Δi_2 generated by clamp 2 in order to keep $E_2 = E$ during ΔE_1, and from the transjunctional voltage difference $E_j = E_1 - E_2 = \Delta E_1$, g_j is calculated as $-\Delta i_2/\Delta E_1$. At any given E several such voltage pulses ΔE_1 were made, to ensure that g_j was measured in steady state. All g_j values in the text thus are steady-state chord conductances.

Nonjunctional membrane resistance, r_1, of the cell receiving the test voltage step was calculated as $\Delta E_1/(\Delta i_1 + \Delta i_2)$.

Junctional conductance in *Chironomus* cell pairs can be very high, on the order of 10 μS, as compared with nonjunctional membrane conductance, which is on the order of 0.1–0.5 μS. This places special demands on the voltage clamps and on the microelectrodes since large currents are required to develop and maintain a voltage difference ΔE across this conductance. We therefore used electrodes with low resistances, about 15–20 MΩ for *e*, and 8–15 MΩ for *i* electrodes, to increase

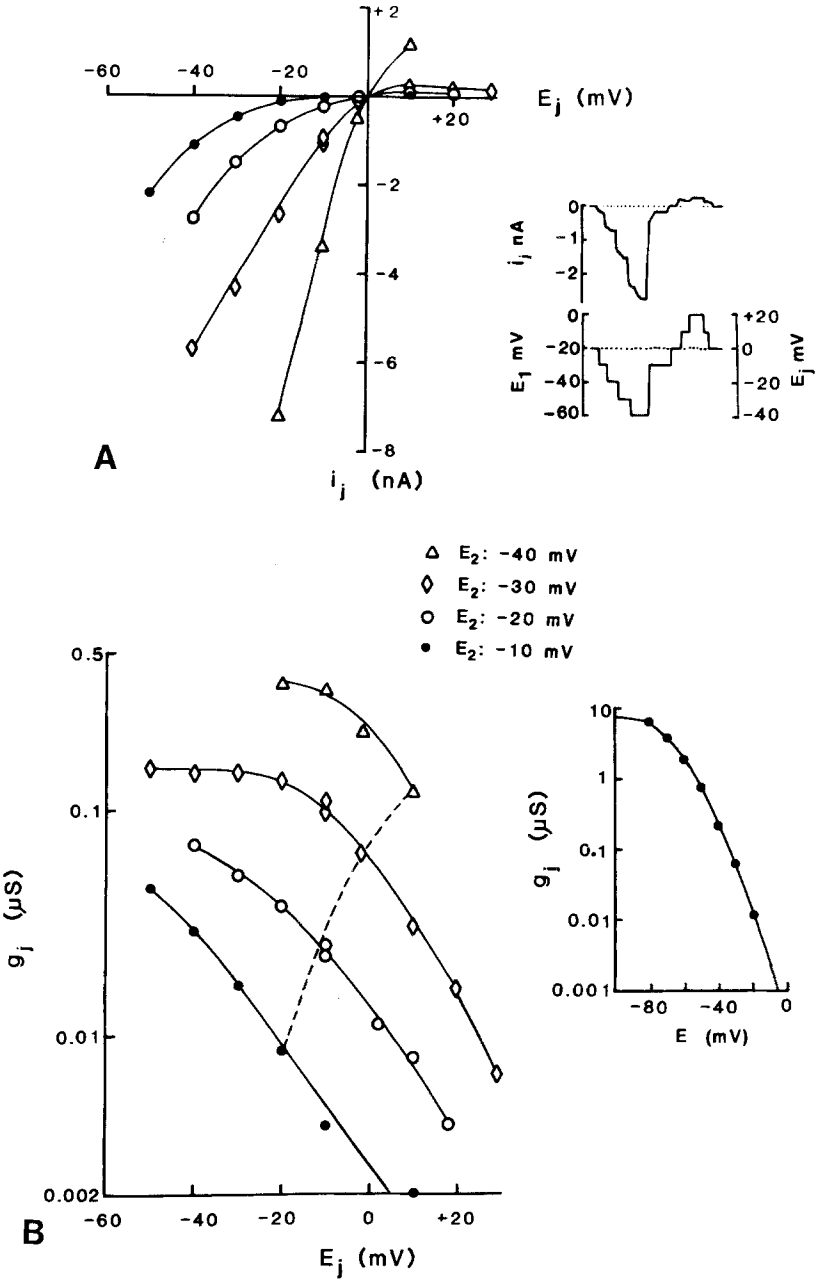

Fig. 3. Does transjunctional potential specify g_j? In this experiment, one cell of a pair was clamped at a particular potential E_2, while the other cell's potential (E_1) was moved in staircase fashion (*Inset*) to potentials more negative or positive than E_2. *(A)*: Plot of the steady-state junctional currents i_j measured at various potentials E_1, *vs.* transjunctional potential $E_j = E_1 - E_2$, for 4 different E_2: −40 mV (△); −30 mV (◇); −20 mV (○); −10 mV (●). The more negative E_2, the larger was i_j at any given E_j, suggesting that cell membrane potentials rather than the transjunctional potential determine g_j. *Inset:* Chart record tracings of E_1 and i_j from this experiment, for $E_2 = -20$ mV (dotted line). *(B)*: Plot of g_j, calculated from the data in *A*, *vs.* E_j. Dashed line is drawn through points with $E_1 = -30$ mV. *Inset:* Plot of g_j *vs.* E ($E_1 = E_2$) of the same junction (filled circles); the curve was calculated according to Eq. (4) based on $g_j \max = 8$ μS ($r = 0.999$), $A = 0.081$ mV^{-1}, $E_0 = -59.8$ mV. All other curves in this figure were drawn by eye

the electrodes' current capacity and the effective gain of the clamps. Nonetheless, it was often impossible to achieve adequate clamping of cell 2, i.e., to maintain $E_2 = E$ during ΔE_1, so that even at the highest practical clamp gain cell 2 experienced a potential shift ΔE_2. In these cases, we approximated g_j as $-\Delta i_2/(\Delta E_1 - \Delta E_2)$. To assess the error of these g_j determinations, especially under conditions of large g_j, we used a cell-pair equivalent circuit with resistors of known values, and calculated g_j as $-\Delta i_2/(\Delta E_1 - \Delta E_2)$ at various clamp gains for various r_j and r_1, r_2 (nonjunctional membrane resistances) in the circuit. In the worst cases, at effective clamp gains so low that $\Delta E_2 = 60$–75% of ΔE_1, the error in determining r_j was 28% for $r_j = 20$ kΩ, 24% for $r_j = 80$ kΩ, 16% for $r_j = 396$ kΩ, and 8% for $r_j = 5$ MΩ (all with $r_1 = r_2 = 1$ MΩ). With higher r_1 and r_2 (9 MΩ, closer to values commonly encountered), the errors were lower: 18% for $r_j = 20$ kΩ, 8% for $r_j = 80$ kΩ, 4% for $r_j = 396$ kΩ, 2% for $r_j = 1$ MΩ, and 1% for $r_j = 5$ MΩ. The important point is that the error is large only near the plateau of the g_j *vs.* E curves, and this would affect mainly the apparent $g_j \max$ values (*see* Results). Since, in data analyses, $g_j \max$ was determined by curve fitting, where a good fit to points away from the plateau was considered critical, these errors do not significantly affect either our general results or their interpretation.

Injection of Ca^{2+} or EGTA

For intracellular injections by either pressure or iontophoresis, an additional capillary was inserted into one cell. For iontophoresis, the capillary was connected to an independent current source with current return via the bath.

pH_i Measurements

For intracellular pH measurements we manufacture pH-sensitive glass microelectrodes according to Thomas (1974), using the same equipment, calibration, and selection procedure as described before (Rose & Rick, 1978). We are grateful to Roger Thomas for a gift of several pH-microelectrodes during the summer of 1980.

Results

Effect of Membrane Potential on Junctional Conductance

After impalement by all four microelectrodes, cell pairs in "TC-medium" had resting potentials ranging −10 to −40 mV. Usually, the two cells' potentials were nearly equal. Membrane resistances r_1, r_2 ranged 1–8 MΩ. When we set membrane potential E at various, but for the two cells equal, levels, we found junctional conductance g_j to vary with E. Plotted against E, g_j described a sigmoid curve: at rather negative potentials, g_j tended asymptotically toward an upper limit, g_j max; with increasing cell depolarization, g_j fell by several orders of magnitude, approaching a zero asymptote (Fig. 2*A* is a semilogarithmic presentation of the data). With sufficient depolarization, g_j was always reducible below our limit of resolution (i.e., less than 10 nS in the usual recording condition), and reversibly so. In "TC-medium," g_j max of the various cell pairs ranged 4–30 μS (10 junctions).

When E_1 and E_2 are varied independently, it becomes evident that g_j depends on each cell's membrane potential and that it is not specified by transjunctional potential E_j $(=E_1-E_2)$. This was seen when one cell of a pair was clamped at a fixed potential (E_2) and the other, in staircase fashion, to a progression of potentials (E_1) different from its partner's potential (*see* Inset, Fig. 3*A*). The steady-state junctional currents i_j corresponding to the individual potentials E_1, were recorded. This protocol was repeated for several different fixed potentials E_2. In Fig. 3*A*, the junctional currents are plotted against the corresponding transjunctional potentials. It is clear that for any given E_j the junctional current i_j varies with E_2. In Fig. 3*B* the g_j values calculated from the data in *A* are plotted against E_j. Comparing the g_j's for a given E_j, we find that: (1) g_j varies with E_2, *viz.*, is larger the more negative the unvarying potential. Thus, whatever influence E_j may have on g_j, it clearly does not determine it uniquely. (2) Within each set of measurements, g_j declines as E_1 (and hence E_j) becomes more positive, and it rises toward a plateau as E_1 is made more negative

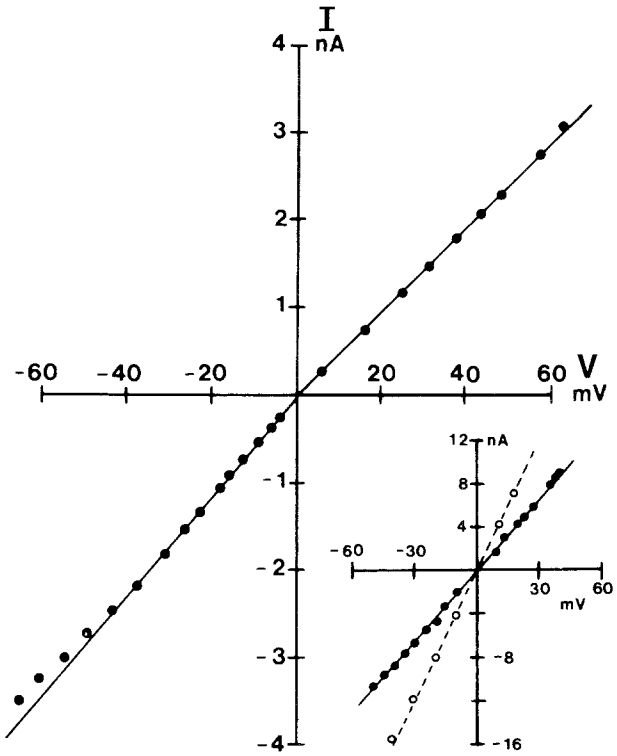

Fig. 4. Current-voltage characteristic of nonjunctional membrane. An isolated single cell bathed in "TC-medium" was voltage clamped to various potentials ($E_{rest}+V$) more negative or positive than resting potential ($E_{rest}=-30$ mV). The plot of the voltage clamp steps V *vs.* the clamp current i is essentially linear over the membrane potential range −90 to +30 mV, with only a small difference in slope (i.e., conductance g) for outward currents ($g=48$ nS) and inward currents ($g=59$ nS) in this cell. *Inset: I–V* curve of another single cell ($E_{rest}=-30$ mV) has a slope of 220 nS in "TC-medium" (filled circles). The slope is approximately doubled in "K_2SO_4-medium" (open circles, $E_{rest}=-2$ mV), but the characteristic remains linear. Resting potentials are the origins of abscissae in all cases of this figure

– a plateau whose height apparently increases with negativity of the fixed potential E_2. (3) If, instead of focussing on the solid lines drawn in Fig. 3*B*, we connect points of equal E_1 (e.g., broken line, Fig. 3B), we generate a set of curves representing the variation of g_j *vs.* E_2 for (various) fixed E_1. The two sets of curves suggest mirror-symmetry about the line $E_j=0$. Thus, the asymmetry of the solid curves about $E_j=0$, rather than indicating an asymmetric junction, means only that $|E_j|$ is not the determinant of g_j.

Effect of Membrane Potential on Nonjunctional Membrane Conductance

The potential-dependent conductance change just described is particular to the junction; nonjunctional membrane conductance stays constant over

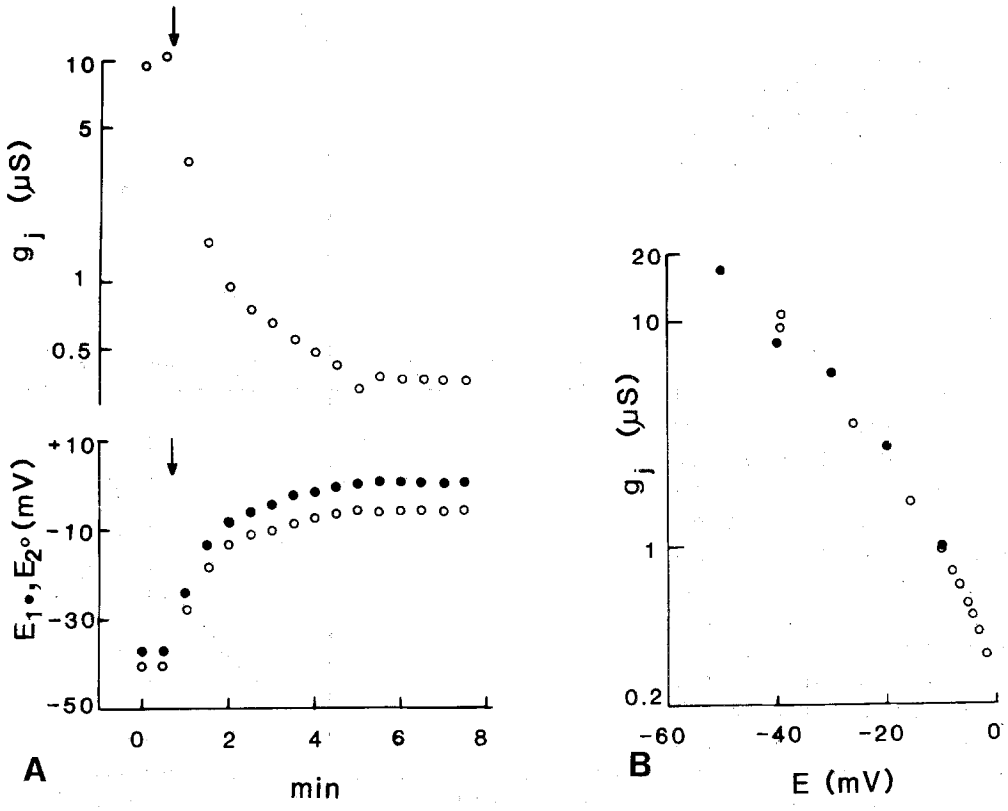

Fig. 5. Effect on g_j of cell depolarization by K-medium. *(A):* Time course of changes in cell potential and junctional conductance during replacement of "TC-medium" with "K_2SO_4-medium." g_j was determined at various instantaneous cell potentials set by the increasing K:Na ratio in the bath during the medium exchange begun at the arrow. *(B):* Plot of g_j *vs.* the corresponding instantaneous membrane potentials E. Since there was a small difference between E_1 and E_2, we plot $(E_1+E_2)/2$ (open circles). After a steady membrane potential had been reached (indicating complete medium exchange), the cells were clamped to various potentials E ($E_1=E_2$), and the corresponding steady-state g_j's were determined, filled circles. The two sets of measurements fall on the same curve, indicating that g_j is determined by membrane potentials rather than by nonjunctional currents introduced by the clamps. Depolarizations with "K-Melnick's" gave the same results

a wide range of membrane potential. To establish this point, we voltage clamped isolated single cells to various potentials more negative or positive than their resting potentials and measured the corresponding steady-state membrane currents (I–V characteristic). The cells had resting potentials of -20 to -40 mV in "TC-medium." Their I–V characteristic was essentially linear over the membrane potential range of -90 to $+40$ mV (Fig. 4); and thus nonjunctional membrane conductance, g, (ranging 0.05 to 0.2 μS for the various single cells) is nearly independent of membrane potential over this range. (In some cells, the slope of the curve associated with inward currents was slightly larger than that associated with outward currents; *see*, e.g., Fig. 4.) The fact that g is independent of membrane potential suggests that there are very few, if any, potential-sensitive ion channels in the nonjunctional membrane of these epithelial cells.

Junctional Conductance Depends on Membrane Potential, Not on Membrane Currents

Since, during voltage clamping to the various membrane potentials, currents are necessarily driven through the nonjunctional cell membranes, the possibility arises that g_j changes are a result of these currents rather than of the changes in membrane potential associated with them. Therefore we depolarized cell pairs by exchanging the usual Na- for a K-medium, and measured g_j *vs.* E during the exchange (Fig. 5). The g_j values, measured at the potentials set entirely by K^+ concentrations and those obtained at voltage-clamped potentials of the same cell pair after completion of the Na-for-K exchange, fall on the same curve (Fig. 5*B*), implying that g_j is determined by membrane potentials and not by membrane currents.

The invariance of $g_j(E)$ when "TC-medium"

is replaced by "K_2SO_4-medium" shows that neither Na^+ nor Cl^- is required for mediating E-dependent changes in g_j (Fig. 5*B*).

Analysis of Voltage Dependence

In principle the cell-to-cell conductance, g_j, can be considered as the sum of conductances of all the cell-to-cell channels plus any "leak" conductance not of cell-to-cell channel origin. In the case of *Chironomus,* the leak conductance is negligible. (For example, in Fig. 3*B* it must be $<0.03\%$ g_j max.) A change in g_j could then be the result of a change in number of open channels, a change in single (open) channel conductance, or both. We make the assumption that a decrease (increase) in g_j signifies a decrease (increase) in the number of open channels.

As noted above, several kinds of experiments have indicated that g_j can be modified from either side of a junction, that is, from either cell partner. Given that each cell-to-cell channel is made of two hemichannels, one associated with each cell, this suggests the possibility that each hemichannel contributes a separate gate or set of gates that effect(s) channel closure in response to Ca^{2+}, to H^+, and to depolarization on its side of the junction. This notion is supported not only by the apparently interchangeable roles of E_1 and E_2 (for example, in the experiment of Fig. 3), but also by the limiting, or bounding, effect that either cell's potential appears to impose when we try to increase g_j by making the other cell very negative. Specifically, the progression of g_j plateau heights in Fig. 3*B* suggests that *each* cell's influence on g_j enters a plateau range as the cell is made sufficiently negative; that we can approach g_j max only when both cells enter their "plateau" ranges; that when either E is outside its "plateau" range it has a limiting effect on g_j that we cannot override no matter how negative we make the other E; but that, within the resolution of our measurements, neither E appears to impose a lower limit on g_j. Collectively these features suggest that g_j can be expressed as a product of an E_1-dependent function and an E_2-dependent function, both of similar form.

To model the voltage dependence of g_j, we then assume (1) that all channels in a junction are alike[1]; (2) that each has two gates in series, one associated with each cell face of the junction; (3) that these gates are independently controlled; and (4) that under constant conditions the gates on a given junction face are in an equilibrium distribution between open and closed states, a distribution that depends on that side's membrane potential in the way envisaged in a conventional physical model (*see* Ehrenstein & Lecar, 1977). Hence, the conductance g_j of a junction is the resultant of two independent thermodynamic equilibria of this sort – that is, one in each of its associated gate populations – expressible as a compound probability. Using parentheses to indicate functional relations, we may write

$$g_j(E_1, E_2) = N\gamma_j f_{o1}(E_1) f_{o2}(E_2) \tag{1}$$

where N is the total number of channels; γ_j, the single-channel conductance; $f_{o1}(E_1)$, the fraction of gates open at equilibrium in the population in junction face 1, and $f_{o2}(E_2)$, the corresponding fraction (probability) in junction face 2.

The factors $f_{o1}(E_1)$ and $f_{o2}(E_2)$ are expressed in terms of the Gibbs free energy of the opening process. (Appendix 1 reviews the conventional model, in which the free energy change is related to a presumptive change in dipole moment of a membrane voltage sensor.) At equilibrium,

$$f_{o1}(E_1) = \left(1 + \exp \frac{\Delta G_1^\circ + zFE_1}{RT}\right)^{-1}$$
$$f_{o2}(E_2) = \left(1 + \exp \frac{\Delta G_2^\circ + zFE_2}{RT}\right)^{-1}, \tag{2}$$

where ΔG° is the standard chemical free energy per mole for the process; z is the equivalent number of elementary electric charge units presumed to traverse the potential difference E to effect opening (and often called the "gating charge"); F is the Faraday constant; R is the gas constant; T is the Kelvin temperature; and subscripts 1 and 2 refer to the respective gate populations on the two junction faces and to their associated cell membranes. Formally we may write $\Delta G_i^\circ = -zFE_{0i}$, where E_{0i} is the potential at which half the gates on junction side i ($i=1$ or 2) are open. Then,

$$f_{oi}(E_i) = \{1 + \exp[A(E_i - E_{0i})]\}^{-1} \tag{2a}$$

where $A = zF/RT$ expresses the voltage sensitivity of the gates (*cf.* Labarca, Coronado, & Miller, 1980). Now, referring to Eq. (1), we designate by $n_o = Nf_{o1}f_{o2}$ the number of open *channels;* and by $g_j \max = N\gamma_j$ the upper limit of $g_j(E_1, E_2)$.

[1] The model would apply equally if the single channel conductance in the open state varied from channel to channel, as long as all gates in a given junction face had identical voltage response characteristics. Then γ_j in Eq. (1) would represent the mean open-state conductance for the whole population of channels in a junction.

It follows that

$$\frac{N}{n_o}=\frac{g_j\max}{g_j} \tag{3}$$
$$=\{1+\exp[A(E_1-E_{01})]\}\ \{1+\exp[A(E_2-E_{02})]\}.$$

We now consider experiments such as that of Fig. 2, where both cells of a junction were treated equally: they were exposed to the same media, and their potentials were clamped to equal values ($E_1=E_2=E$) except for the small, brief test pulses. Taking the gates for both cells to be identical, we assume, in analyzing these experiments, that $E_{01}=E_{02}=E_0$. Then

$$g_j\max/g_j=[1+e^{A(E-E_0)}]^2 \tag{4}$$

and

$$\log[\sqrt{g_j\max/g_j}-1]=\frac{A(E-E_0)}{2.3}. \tag{5}$$

The plot g_j *vs.* E predicted by Eq. (4) is sigmoidal, with its position along the E axis defined by E_0, and with its slope at $E=E_0$ proportional to A and to $g_j\max$. A plot of $\log[\sqrt{g_j\max/g_j}-1]$ *vs.* E should then be linear, with a slope of $A/2.3$, from which we can calculate $z=ART/F$ and E_0, the potential at which $\sqrt{g_j\max/g_j}-1=1$, i.e., at which half the gates on each junction face are open.

To determine $g_j\max$ for a set of g_j *vs.* E data, we estimate the apparent plateau value from a plot of g_j *vs.* E. We use this and other trial values differing by increments of about $\pm 10\%$ to determine, by linear regression, the $g_j\max$ that best fits Eq. (5) to the data. We adopt the value of $g_j\max$ that yields the highest correlation coefficient (r). A difference of 10% in the choice of $g_j\max$ can give rise to as much as a 20% difference in the estimate of A.

The data of Fig. 2*A* are analyzed in this manner. Figure 2*B* (open circles) presents the plot according to Eq. (5). When we use $g_j\max=30$ μS, the data are well fit by a straight line ($r=0.996$) whose slope gives $A=0.077\ \mathrm{mV}^{-1}$, and $E_0=-27.2$ mV. With $g_j\max$, A, and E_0, we can calculate g_j at any given E according to Eq. (4). The solid line of Fig. 2*A* represents the calculated g_j *vs.* E curve, which describes the data well. For the various cell pairs tested ($n=10$) in "TC-medium" shortly after their isolation, $g_j\max$ ranged 3 to 30 μS; A, 0.077 to $0.085\ \mathrm{mV}^{-1}$ (corresponding to a z range of 2.0–2.2); and E_0, −10 to −35 mV.

We get similar results with cell pairs isolated surgically from the gland.

So far, we have shown that the model described by Eq. (3) is valid when $E_1=E_2$. We tested whether it also accounts for g_j when $E_1\neq E_2$. To this end, we first determined the g_j *vs.* E relation for a cell pair with $E_1=E_2=E$, and then measured steady-state g_j values for several $E_1\approx -E_2$ (and hence for several E_j). From the g_j *vs.* E curve based on 16 data points (Fig. 12, *Inset*), we evaluated $g_j\max$ (19 μS; $r=0.992$), A ($0.073\ \mathrm{mV}^{-1}$), and E_0 (−28.2 mV). In Table 1, the g_j values for $E_1\approx -E_2$ are compared with values calculated according to Eq. (3) for the corresponding E_1, E_2. We see that the model in Eq. (3) accounts for $g_j(E_1, E_2)$ here just as it does when $E_1\approx E_2$ (e.g., Fig. 2). In particular, g_j is accounted for in terms of a product $f_{o1}(E_1)f_{o2}(E_2)$ (*see* Eq. (1)) even when $E_j\neq 0$ (E_j here ranged 22 to 58 mV!).

Table 1. Junctional conductance in the presence of transjunctional potential

E_1 (mV)	E_2 (mV)	$\lvert E_j\rvert$ (mV)	Observed g_j (μS)	Calculated g_j (μS)
−28	+30	58	0.138	0.133
−19	+20	39	0.179	0.185
−10	+12	22	0.155	0.200

Application of the model to the case $E_1\neq\pm E_2$, as in Fig. 3, is considered in the Discussion.

Effect of Ca^{2+} and H^+ on g_j and on Its Potential Dependence

Elevation of the intracellular concentration of either Ca^{2+} or H^+ has been shown to decrease junctional conductance in *Chironomus* as well as in other animal cells (Ca^{2+}: Rose & Loewenstein, 1976; Dahl & Isenberg, 1980; Spray et al., 1982*a*, *b*; for further references, *see* Loewenstein & Rose, 1979; but *see also* Johnston & Ramon, 1981. H^+: Turin & Warner, 1977, 1980; Rose & Rick, 1978; Spray et al., 1979, 1982*a*, *b*; but *see also* Johnston & Ramon, 1981). In *Chironomus* salivary gland, elevation of either $[Ca^{2+}]_i$ or $[H^+]_i$ causes cell depolarization (Rose & Loewenstein, 1976; Rose & Rick, 1978). Hence, two questions arise: (1) do these ions affect g_j only via their depolarizing action or also by another mechanism? and (2) how does Ca^{2+} or H^+ influence the g_j *vs.* E relation?

Ca^{2+}. We found that $[Ca^{2+}]_i$ elevation effects g_j even when depolarization is prevented: Ca^{2+} injection into voltage clamped cells reduced g_j (Fig. 6). This finding confirms earlier results with clamped salivary gland cells, but where electrical coupling rather than g_j was measured (Rose & Loewenstein, 1976).

A qualitative answer to the second question is given by experiments in which, following Ca^{2+} injection, hyperpolarizations by clamping raised the depressed g_j reversibly (Fig. 6, data at arrows).

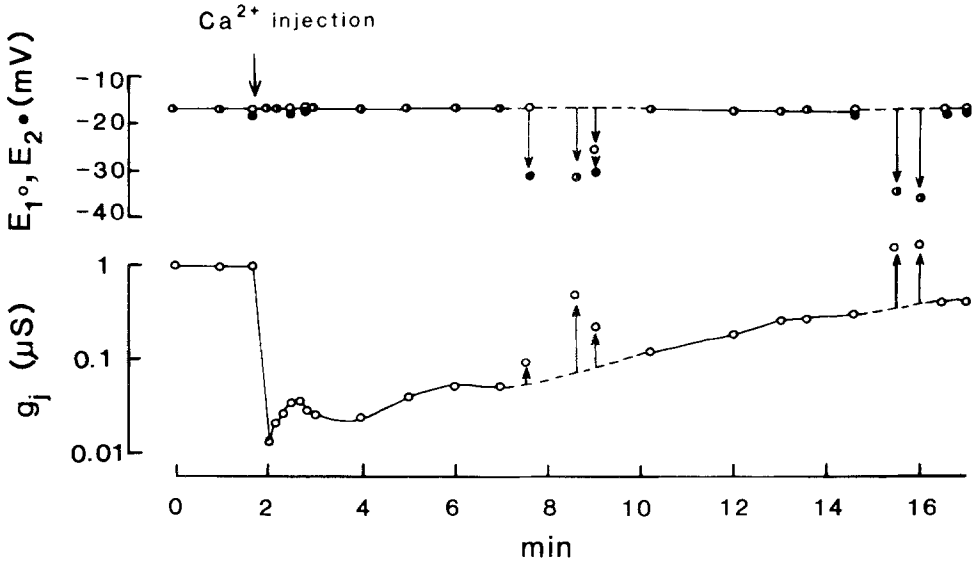

Fig. 6. Effect of $[Ca^{2+}]_i$ elevation on g_j at fixed membrane potentials. g_j was determined during $[Ca^{2+}]_i$ elevation while cells of the pair were clamped at their resting potentials. Ca^{2+} injection (0.18 M $CaCl_2$, 0.1 M KCl, pH 7.4 with KOH; by pressure, at first arrow) into cell 1 rapidly reduced g_j which then gradually recovered with time. Transient hyperpolarizations by voltage clamping (E at arrows) resulted in reversible g_j increases, persisting during the hyperpolarization (data at arrows). Hyperpolarization of the uninjected cell alone (first arrow after injection) increased g_j only little as compared with hyperpolarization of both cells

Clearly g_j remains sensitive to E here. Because of continuous Ca^{2+} pumping by the cell, Ca^{2+} injection is not likely to result in a $[Ca^{2+}]_i$ elevation that is both moderate and stable long enough (i.e., $\gtrsim$10 min) to permit an adequate characterization of the g_j *vs.* E relation. To realize such a condition, we poisoned the cells with NaCN. This causes $[Ca^{2+}]_i$ to increase (Rose & Loewenstein, 1976) without a concomitant elevation of $[H^+]_i$ (Rose & Rick, 1978). In the experiment of Fig. 7*A*, we first determined the g_j *vs.* E relation in control condition (filled circles). The clamps were then set at the cells' resting potential, and NaCN was applied. This caused g_j to fall from 1 μS to a stable 0.02 μS (dashed arrow). With the cells in CN^- medium, their E was raised to various levels and the corresponding g_j's were determined (open circles). Again the data are accounted for by Eq. (4). This can be appreciated from their good fit to the solid lines that were calculated from the parameters $g_j$max, E_0, and A, evaluated as above. We see further that exposure to CN^- ($[Ca^{2+}]_i$ elevation) shifted the g_j *vs.* E curve to more negative values but had little or no effect on either $g_j$max or the slope of the curve.

We experimented with lowered $[Ca^{2+}]_i$, too. For this, we injected EGTA, a powerful Ca^{2+} chelator (Fig. 7*B*). The protocol here was as follows: (1) the g_j *vs.* E relation was obtained in control condition (filled circles); (2) the clamps were set at −20 mV and cell 1 was injected with EGTA, pH 7.2. Within several minutes g_j rose from 0.86 μS to a stable 2.0 μS (dashed arrow); (3) the g_j values depicted by open circles were determined; (4) EGTA was injected into cell 2; this caused no significant g_j change. Apparently – if we may take g_j as a measure of $[Ca^{2+}]_i$ – the second injection did not lower $[Ca^{2+}]_i$ further. This one might expect if EGTA in the first injection had equilibrated through the open channels. (5) Again, g_i values (open triangles) were determined. They fall sensibly on the same curve as the open circles. Figure 7*B* shows both the data and the curves calculated according to Eq. (4) with the parameters derived from the data's analysis. It can be seen that again the data are accounted for by the model and that the effect of the presumed $[Ca^{2+}]_i$ lowering was a shift of the g_j *vs.* E curve to more positive E, just as $[Ca^{2+}]_i$ elevation had shifted it to more negative E. And again neither $g_j$max nor the curve's slope was affected.

H^+: The analogous experiments with H^+ gave the same answers: $[H^+]_i$ elevation reduces g_j even when cell depolarization is prevented, and its effect on the g_j *vs.* E relation is a shift of the curve to more negative E.

To elevate $[H^+]_i$, we exposed cells to "propionate medium" at pH 6.8. In preliminary experiments we had found that this lowers pH_i from the normal 7.4 to about 6.5. As shown in Fig. 8, propionate treatment lowered g_j from 0.32 μS

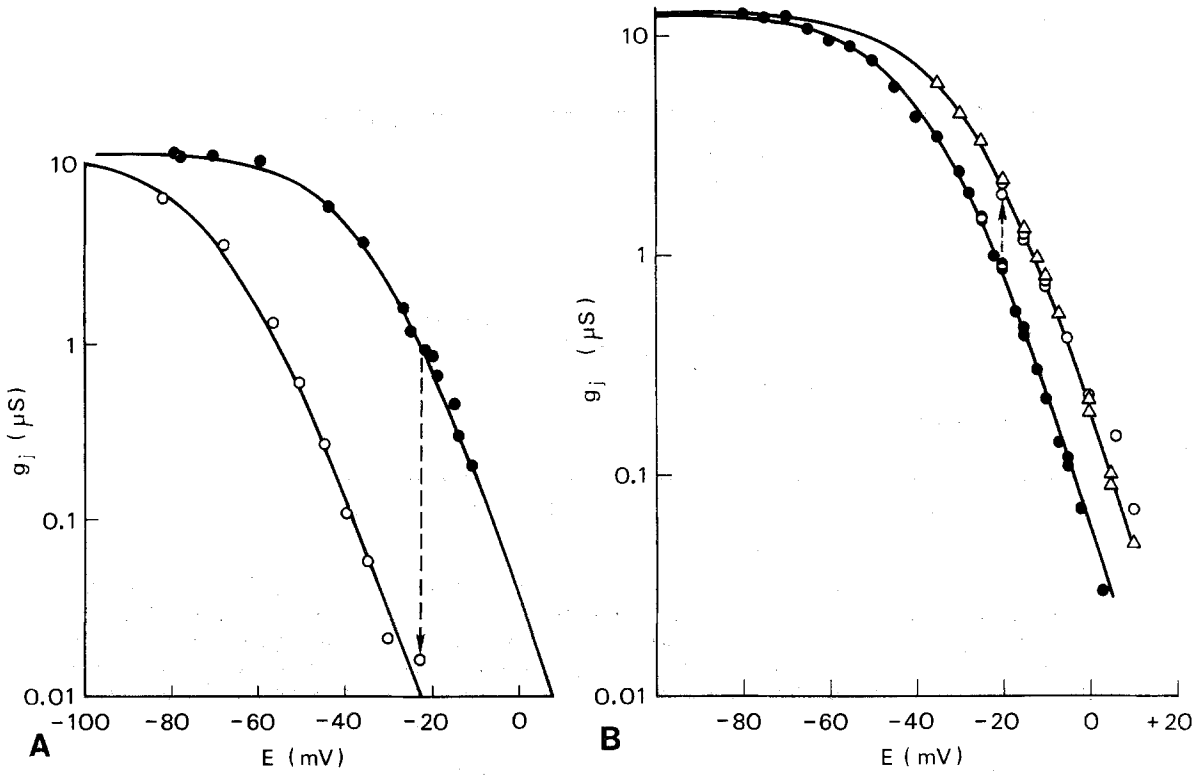

Fig. 7. Effect of changes in $[Ca^{2+}]_i$ on the g_j *vs.* E relation. *(A):* Effect of CN^- exposure (and presumably of $[Ca^{2+}]_i$ elevation). The g_j *vs.* E relation of a junction was first determined in "TC-medium" (control, filled circles). The cell pair was then clamped at −24 mV and exposed to 5 mM NaCN in "TC-medium," which lowered g_j from 1 μS to a stable 0.02 μS within 25 min (arrow). The g_j *vs.* E relation depicted by the open circles was then determined, with the cells still in CN^--medium. (During CN^- experiments, the superfusion pump was left running continuously because the effect reverses rapidly as HCN escapes from the open dish.) Both sets of data were analyzed according to Eq. (5) of the text, with $g_j$max = 12 μS giving the best fit in both cases. From this, we obtained the following parameters of the control and CN^- data, respectively: $r = 0.995$, 0.997; $A = 0.085$, 0.078 mV^{-1}; $E_0 = -33.5$, −67.4 mV; $z = 2.2$, 2.0. The solid lines represent Eq. (4) of the text, calculated with above parameters for control and CN^-, respectively. *(B):* Effect of EGTA injection (and presumably of lowering $[Ca^{2+}]_i$) on the g_j *vs.* E relation. The g_j *vs.* E relation of a cell pair was first determined in "TC-medium" (control, filled circles). EGTA was then injected by pressure (0.4 M EGTA; pH 7.2 with KOH) into cell 2 while cells were clamped at −20 mV. (Injections were clearly visible by the changing refraction they produced within the cell.) This increased g_j in the course of 5 min from 0.86 μS to a stable 2.0 μS (arrow). The g_j values represented by the open circles were then obtained. Subsequent injection of EGTA into cell 1, with cells again clamped at −20 mV, did not significantly change g_j (2.2 μS). The g_j values depicted by open triangles were then measured. Both sets of data obtained after EGTA injection were analyzed together according to Eq. (5) of the text, which resulted in the following parameters, obtained with $g_j$max = 13 μS for best fit: $r = 0.9956$; $A = 0.077$ mV^{-1}; $E_0 = -25.2$ mV. The corresponding parameters for control were: $g_j$max = 13 μS; $r = 0.9963$; $A = 0.079$ mV^{-1}; $E_0 = -34.2$ mV. The curves represent Eq. (4) calculated with above parameters, before and after EGTA injection, respectively

(open triangle) to a stable 0.012 μS (open circle at arrow). Analysis of the g_j *vs.* E data then obtained in "propionate medium" (open circles) shows that the voltage sensitivity A (0.070 mV^{-1}) is similar to that of control experiments (0.077–0.085 mV^{-1}), but that E_0 (−63 mV) is much more negative than ever observed in controls (−10 to −35 mV). Upon washout of propionate, which raises pH_i to 7.4 or higher, the g_j *vs.* E relation shifted back to more positive E (filled circles, dotted curve).

Ca^{2+} and H^+ ions thus determine the position of the g_j *vs.* E curve along the voltage axis, but neither $g_j$max nor A is affected by either ion (at moderately elevated concentrations).

Channel Closures by Ca^{2+} or H^+ that are Not Reversible by Hyperpolarization

The experiments of Figs. 6, 7*A* and 8 show that during elevation of $[Ca^{2+}]_i$ or $[H^+]_i$ g_j can be restored by clamping cells to more negative values. In some instances (e.g., Fig. 9) where g_j was sensibly abolished by lowering of pH_i (cell exposure to medium saturated with 100% CO_2) or pCa_i (Ca^{2+} injection), no restoration of g_j was detect-

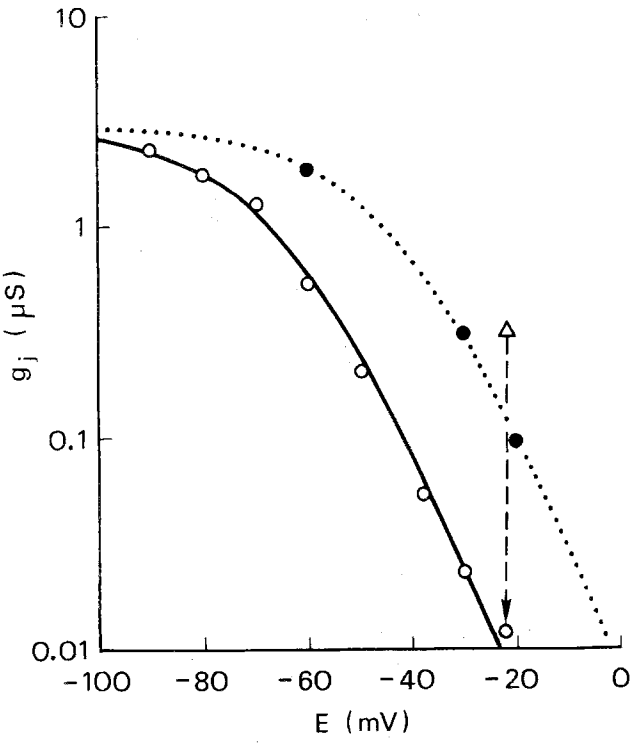

Fig. 8. Effect of "propionate" medium (and presumably of pH_i decrease) on voltage dependence of g_j. A cell pair was clamped at −22 mV. Upon application of "propionate" medium, g_j at that E fell from 0.32 μS (triangle) to a stable 0.012 μS (open circle at arrow). Open circles: g_j *vs.* E relationship in "propionate medium" (which, as measured in other experiments, lowers pH_i to about 6.5). Filled circles: data collected about 30 min after "propionate medium" was replaced with "TC-medium." Analysis of data: with g_j max = 3.0 μS for both sets of data for best fit, we obtained for "propionate medium" A = 0.070 mV^{-1}, z = 1.8, E_0 = −63 mV, r = 0.996, and after washout of propionate, A = 0.071 mV^{-1}; z = 1.8; E_0 = −41 mV, r = 0.999. From these parameters, the curves were calculated

able when both E_1 and E_2 were clamped at potentials as negative as −70 or −80 mV; yet g_j subsequently recovered spontaneously, presumably upon recovery of normal pH_i (Fig. 9) or pCa_i.

One possible interpretation of these results is that the high value of $[H^+]_i$ or $[Ca^{2+}]_i$ attained here shifted E_0 to very negative values. An alternative interpretation is that each *hemi*channel contributes two gates in series, one responsive to voltage, the other voltage-insensitive but subject to closure by relatively low-affinity binding of Ca^{2+} or H^+.

Does Membrane Potential Alter Either $[Ca^{2+}]_i$ or $[H^+]_i$?

As is clear from the foregoing results, the effect of Ca^{2+} and H^+ on g_j is not mediated by obligatory membrane depolarization.

On the other hand, the sensitivity of g_j to potential could be mediated by Ca^{2+} or H^+ if membrane potential were a controlling factor for the cytosolic activity of either or both ions. Since Ca^{2+} or H^+ elevation decreases g_j, such a control would have to upregulate the concentration of these ions with decreasing negativity of potential and downregulate it with increasing negativity. In principle, this could be brought about either by potential-dependent changes in net influx rate of these ions across the plasma membrane or by potential-dependent release/uptake by an intracellular store.

Ca^{2+}. Arguing against the first possibility, in the case of Ca^{2+}, is the finding that the potential dependence of g_j is essentially unaltered by removal of external Ca^{2+}. This was shown by experiments in which cell pairs were kept for periods of up to 1 hr in medium containing 20 mM EGTA (for pH 7.4, we estimated $[Ca^{2+}] \sim 10^{-8}$ M). We then determined the g_j *vs.* E relation and found it just about the same as that obtained at 10,000-fold higher, i.e., at the normal (millimolar), concentration of external Ca^{2+}. In two experiments with 20 mM EGTA, where E was varied between −60 and +10 mV, A was 0.084 mV^{-1}, and E_0 was −18 and −20 mV.

However, Ca^{2+} could conceivably be released/taken up in a potential-dependent manner by an intracellular store. In that case, exhaustion of the Ca^{2+} store should abolish the sensitivity of g_j to depolarization. In an effort to deplete such a Ca^{2+} store, we first exposed a cell pair for 1 hr to 5 mM EGTA and then injected EGTA iontophoretically into each cell (10 nA dc for 31 and 37 min, respectively). This treatment, too, failed to abolish potential dependence of g_j as tested from E = −60 to −5 mV (A = 0.068 mV^{-1}, E_0 = −36 mV). (*See also* Fig. 7*B*, another case of EGTA injection.)

H^+. Since extracellular $[H^+]$ is very low, it is not likely that membrane potential significantly alters pH_i by a direct effect on H^+ flux across the cell membrane, but it might affect cytosolic pH by other mechanisms. We therefore measured pH_i with pH-sensitive microelectrodes during cell potential changes caused either by exposure to K-medium or by voltage clamping. In neither case could we detect a pH_i decrease correlated with depolarization or a pH_i increase correlated with hyperpolarization (5 experiments). In fact, in one experiment, pH_i of a cell increased during depolarization by "K_2SO_4-medium", and yet g_j decreased.

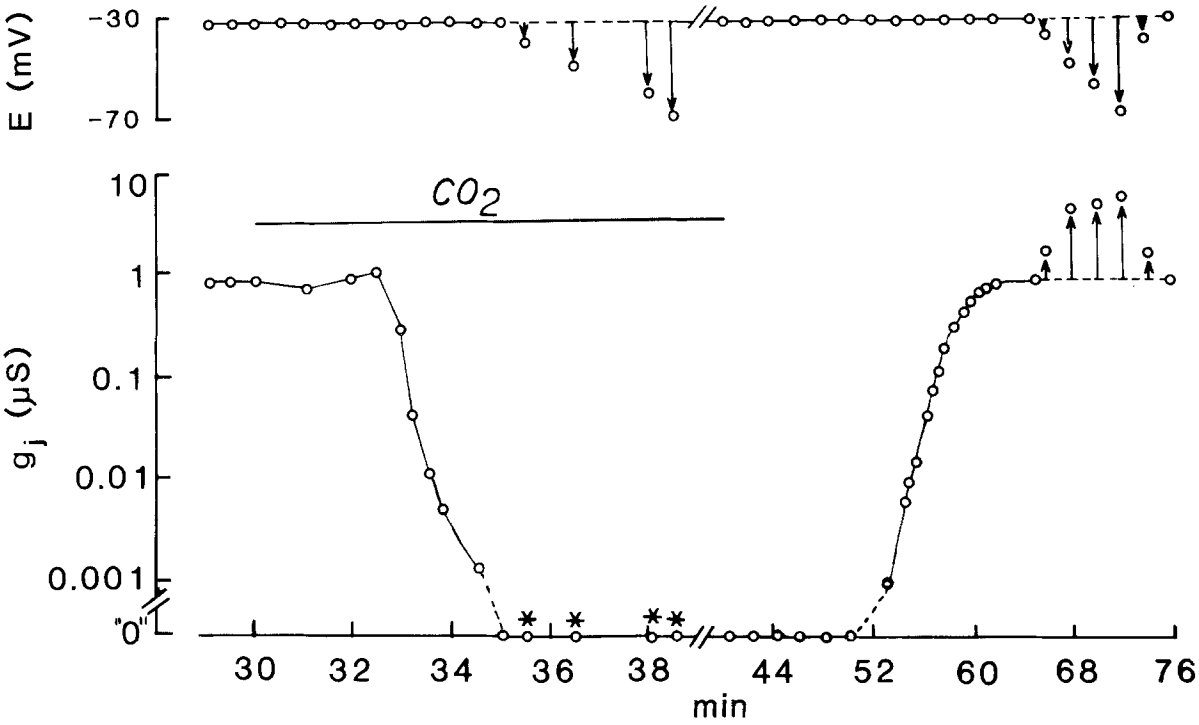

Fig. 9. Drastic lowering of pH_i sensibly abolishes g_j even at fixed membrane potentials: hyperpolarizations fail to regenerate a detectable g_j. The cells of a pair were voltage clamped at −33 mV and g_j was determined during exposure of the cells to "TC-medium" saturated with 100% CO_2. This CO_2 concentration decreases pH_i in *Chironomus* cells to as low as 6.0 (Rose & Rick, 1978). (pH of medium: 6.1. Medium pH as low as 6 has no effect on g_j.) In CO_2-medium, membrane polarizations (arrows) as negative as −70 mV did not detectably increase g_j (corresponding g_j points marked by asterisks). Limit of resolution in this experiment was 0.001 μS; all values below this limit are plotted as "0" μS

Discussion

Dependence of g_j on Membrane Potential Indicates Channels Have Two Independent Gates in Series

We have shown in this study that junctional conductance g_j of *Chironomus* salivary gland cells depends on membrane potential E. When the potentials of the joined cells are equal, g_j *vs.* E describes a sigmoid curve, diminishing asymptotically towards zero as E is made more positive and rising to a plateau for sufficiently negative E. When the cells of a pair are at unequal potentials, the two potentials together determine g_j, but their difference – the transjunctional potential – does not specify it (Fig. 3*B*). When either cell's membrane potential (E_1, E_2) is fixed and the other varied, the fixed potential imposes an upper limit on g_j, though apparently not a lower limit (Fig. 3*B*). Junctional conductance is determined by E, no matter whether this is set by ion concentrations or by voltage clamping. Nonjunctional membrane currents, therefore, are not the cause of the g_j changes observed when cells are clamped to various potentials. The finding that sufficiently positive potentials reduce g_j by three orders of magnitude and below our limit of resolution (*see,* for example, Fig. 3*B* and *Inset*) indicates that all the cell-to-cell channels of a junction are sensitive to membrane potential. The voltage-sensitive junctional conductance contrasts with nonjunctional membrane conductance, which is insensitive to membrane potential over a wide range (Fig. 4). These results explain earlier observations, in which electrical coupling between two contiguous cells in this tissue was seen to decrease when either or both of the cells were depolarized electrically (Politoff, Socolar & Straus, 1970; Socolar & Politoff, 1971) and to increase with hyper- or repolarization (Rose, 1970).

Earlier reports (Rose & Loewenstein, 1971, 1976) that electrical coupling between cells in the (intact) salivary gland is often not sensibly affected by depolarization with K-medium are not in conflict with the present results. The coupling coefficient, V_2/V_1 (the ratio of membrane potential displacements in two cells when a current step is passed between cell 1 interior and the bath), used as an index of g_j in those earlier studies, is not a sensitive measure at high g_j. A 10- to 50-fold reduction of g_j together with the concomitant twofold increase in nonjunctional conductance (*see* Fig. 4, *Inset*) would have reduced V_2/V_1 by about 3–8% in the case of initial $V_2/V_1 = 0.99$ (*see* Socolar, 1977, Fig. 7). Detection of such a small change in V_2/V_1 would have required substantially higher resolution of

V_1 and V_2 than was used in those experiments. Whenever $V_2/V_1 < 0.96$, depolarization by K-medium was, in fact, seen to reduce electrical coupling in those experiments.

The form of the relation $g_j(E)$ is correctly predicted if we treat g_j as the resultant of two independent voltage-sensitive equilibria – that is, as a product of two probability functions, each reflecting the potential of one cell partner of the junction (Eqs. (1) and (3)). Indeed, when $E_1 = \pm E_2$ (and thus even in the presence of a considerable E_j), our experimental results are in excellent quantitative agreement with such a thermodynamic model (*see* Figs. 2, 7, 8, 12 *Inset;* Table 1). This strongly suggests that each cell-to-cell channel has two independent voltage-sensitive gates, and that E, rather than E_j, determines their patency. It is appropriate, however, to ask whether another, equally simple – or simpler – model can also account for our measurements.

Comparison with Other Gating Models

If every channel has only one voltage-sensitive gate, the g_j *vs.* E data in Fig. 2*A* should be accounted for by the equation

$$\frac{g_j \max}{g_j} = 1 + \exp[A(E - E_0)].$$

The latter would imply a linear function of E in the form

$$\log\left(\frac{g_j \max}{g_j} - 1\right) = \frac{A(E - E_0)}{2.3}. \tag{6}$$

In Fig. 2*B*, using the data of Fig. 2*A*, we plot the left side of Eq. (6) as a function of E (filled circles). The obvious nonlinearity, seen consistently in our experiments when the data are plotted in this form, rules out a simple one-gate model.

Another model worth testing is one that endows the channel with two *inter*dependent voltage-sensitive gates, such that each can close only while the other is open. This form of gate constraint has been proposed for explaining results obtained with amphibian embryo cell pairs (Harris, Spray & Bennett, 1981). To examine our data for any such interdependence, we first ask what form of g_j *vs.* E relation such a constraint would generate.

Let n_o be the number of channels in a junction that are open (on both sides), n_1 the number with only the gate on side 1 open, and n_2 the number open only on side 2. If there are N channels altogether, and if no channel can have both its gates closed simultaneously, the ratio of closed to open channels is

$$\frac{N - n_o}{n_o} = \frac{n_1 + n_2}{n_o}.$$

From Eq. (2a), it follows that $n_2/n_o = \exp[A(E_1 - E_0)]$ and $n_1/n_o = \exp[A(E_2 - E_0)]$. Since $g_j \max/g_j = N/n_o$,

$$\frac{g_j \max}{g_j} = 1 + \exp[A(E_1 - E_0)] + \exp[A(E_2 - E_0)].$$

For the case $E_1 = E_2 = E$, this gives

$$\log\left[\frac{(g_j \max/g_j) - 1}{2}\right] = \frac{A(E - E_0)}{2.3}. \tag{7}$$

If no channel can have both its gates closed simultaneously, the data of Fig. 2*A* when plotted according to Eq. (7) should fit a straight line. The filled circles in Fig. 2*B* give such a plot, albeit with each point displaced upward by a constant amount (log 2). The deviation from linearity shows that also the interdependent gate model of Eq. (7) cannot apply to our data.

Thus, at the level of a cell-to-cell channel, we interpret the success of our model, in both the presence and absence of a transjunctional potential, to mean (1) that each channel has two voltage-sensitive gates in series, one associated with each cell partner, or each cell face of a junction; (2) that the two gates can open and shut independently of each other; (3) that the probability for each of the two gates to be open depends on the electrical potential of that gate's associated cell, or junction face (as well as on $p\mathrm{Ca}_i$ and pH_i, discussed further on); and (4) that the probability for a channel to be open is the product of the two independent probabilities that its two gates are open. The reciprocal limiting influences of E_1 and E_2 on g_j (Fig. 3*B*), then, mean that no matter how many gates on one face of the junction are opened by hyperpolarization of the cell on that side, the maximum number of conducting channels can be no greater than the number of gates open on the opposite face of the junction.

Voltage Sensitivity Parameter A: Some Sources of Variance

The value of A, according to the model, should reflect the difference in dipole moments corresponding to open and closed states of the gate (*see* Appendix 1), which, we would prefer to assume, should be a constant. Seemingly unexpected, then, is the degree of variability seen among our experimentally inferred A values (0.068–0.091 mV^{-1}) when we consider the data sets for all experiments, provided they had reasonably well defined $g_j(E)$ curves. Part of the scatter arises from our statistical fit procedure; just the uncertainty in the $g_j \max$ choice can contribute an error as large as 10%. Another component may be attributable to unmatched E_0 values in the cells of a pair.

Indeed, the assumption $E_{01} = E_{02}$ in Eqs. (4) and (5) was made solely for computational convenience. If we use Eq. (3) to predict g_j *vs.* E for $E_1 = E_2$ and $A = 0.08\ \mathrm{mV}^{-1}$, but with E_{01} and E_{02} differing by several tens of millivolts, the result still appears to fit Eq. (5) over an E range similar to that in our experiments. However, the A value derived in such a numerical exercise deviates from the one used in generating the g_j numbers. The size of such deviations leads us to believe that unmatched E_0 values account for at least some – perhaps most – of the differences among A values found in this work. On the other hand, in several experiments where equal polarization of either cell's membrane led to nearly equal g_j, the E_0's appeared to be equal.

The Role of $[Ca^{2+}]_i$ and $[H^+]_i$: Determinants of E_0

The standard free energy for gate opening, and hence its correlate E_0 – that membrane potential ($E_1 = E_2$) at which half the gates on each junction face are open – is rather sensitive to $p\mathrm{Ca}_i$ and pH_i. Moreover, of the three parameters defining a junction's g_j *vs.* E relation, E_0 is the only one affected by moderate alterations in $p\mathrm{Ca}_i$ or pH_i (Figs. 7 and 8); $g_j$max and A remain unchanged under these conditions. However, we also found that more drastic $[\mathrm{Ca}^{2+}]_i$ or $[\mathrm{H}^+]_i$ elevation abolished g_j (<1 nS) even at rather negative E (e.g., Fig. 9).

Taking all these results into consideration, we may infer (1) that *all channels are sensitive to elevation of $[Ca^{2+}]_i$ and of $[H^+]_i$* (*see* footnote 2), *as well as to E* (any of these can reduce g_j to 0); (2) that *all channels shut by moderate elevations of $[Ca^{2+}]_i$ or $[H^+]_i$ can be reopened by E* ($g_j$max is unchanged at elevated $[\mathrm{Ca}^{2+}]_i$ or $[\mathrm{H}^+]_i$); hence, (3) that *Ca^{2+}, H^+ and E all affect the same set of gates*, although neither the ions nor E need act directly on them; (4) that *neither Ca^{2+} nor H^+ modifies the voltage sensor that mediates gate opening/closing* (A remains unchanged). (5) Rather, *it is the location of the g_j vs. E curve along the E axis that is determined by pCa_i and pH_i*; E_0 conveniently specifies this location. The E_0 shift then represents the change in the standard free energy for gate opening, namely the change induced by the alteration in $p\mathrm{Ca}_i$ or pH_i.

Mechanisms for Potential Dependence of g_j

Among the ways E could influence channel patency, we consider the following alternatives: (1) E controls the conformational state and hence the patency of the channel[3]. (2) Channel patency is controlled by the binding of Ca^{2+} or H^+ at the gates or the perichannel membrane (the patch of plasma membrane immediately surrounding each end of the channel) and E controls either (*a*) the binding affinity or (*b*) $p\mathrm{Ca}_i$ or pH_i. It can be shown that under each of these alternatives, the effect of a $p\mathrm{Ca}_i$ or pH_i change could take the form of a simple parallel shift of the g_j *vs.* E curve along the E axis.

As concerns model (2*b*), where E controls $p\mathrm{Ca}_i$ (pH_i), our results rule out control of Ca^{2+} influx by E: we found no significant difference in the E dependence of g_j when extracellular Ca^{2+} was 10^{-8} M rather than the normal millimolar level. But the possibility remains that E modulates the release/uptake of Ca^{2+} by intracellular stores; in our attempts to deplete intracellular stores by using EGTA, we did not monitor $[\mathrm{Ca}^{2+}]_i$ and thus do not know the extent of depletion.

Depolarization, in certain experimental conditions, can indeed raise $[\mathrm{Ca}^{2+}]_i$ in these cells, as demonstrated earlier with the aequorin technique (Rose & Loewenstein, 1976) in salivary glands exposed to K-medium. However, those results do not resolve the present point, because the extracellular medium contained Ca^{2+} there, and, as a further complication, lacked Na^+.

One could envisage a similar mechanism (model 2*b*) involving H^+, in which E controls intracellular concentration of this ion. We saw no evidence of pH changes correlated in a consistent manner with the changes in E; however, the pH electrodes sense pH changes only in their immediate vicinity, and we do not know what happens even a few microns away. In fact, in snail neurons, Roger Thomas (*personal communication*) found a fall in pH_i upon depolarization when the initial pH_i was between 7.2 and 7.4.

An important difference between the models is that in (1) and (2*a*) only *perichannel* membrane potential can be the voltage determinant of channel patency, whereas in (2*b*) the determinant could be

[2] Rose and Rick (1978) had found little reason to believe that H^+ affects g_j on its own. This conclusion was drawn in part from the observed interaction of Ca^{2+} and H^+, and in part from experiments in which cell electrical coupling was affected little or not at all by pH_i changes, or vice versa. The latter conclusion is now no longer cogent in view of the present results; electrical coupling is not always a sensitive indicator of g_j, and, moreover, membrane potential changes may have counteracted the effect of pH_i on g_j, and thus on electrical coupling. This consideration notwithstanding, it remains to be seen whether $[\mathrm{H}^+]_i$ elevation here can effect channel closure on its own (without Ca^{2+} mediation). It is interesting in this connection that only Ca^{2+}, but not H^+ or Mg^{2+}, changes the cell-to-cell channel structure in liver gap junctions (N. Unwin, *personal communication*).

[3] Alternative (1) differs from the others in that it alone allows channel closure to occur without participation of Ca^{2+} or H^+. However, one can imagine this process to be modulated by binding of Ca^{2+} or H^+ (or their mediators) at the hemichannel, binding that alters the free energy of the patency change and thus effects a parallel shift of the g_j *vs.* E curve.

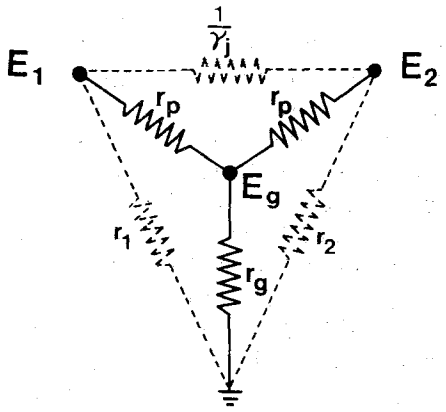

Fig. 10. Lumped element network approximation of perichannel membrane and junctional gap resistances. Diagram refers to a cell pair (membrane potentials E_1 and E_2) linked by one of many (N) parallel cell-to channels (each with resistance $1/\gamma_j$) across a narrow intercellular gap. Each channel incorporates two hemichannels in series; and each hemichannel is embedded in, and crosses, an element of nonjunctional membrane, of resistance r_p. Representing the resistance from the extracellular sides of the perichannel membrane elements, through the intercellular gap to the bulk of the bathing medium, is r_g. Across each perichannel membrane element on the cell 1 face of the junction is the perichannel membrane potential (E_1-E_g); on the cell 2 face, (E_2-E_g). This equivalent circuit is used only for illustrating, semiquantitatively, how the perichannel membrane potential is influenced by the size of r_g (*see* Appendix 2). Shown for reference are r_1 and r_2, representing the nonjunctional (nonperichannel) membrane resistances of cells 1 and 2

the cell membrane potential at large. We cannot measure perichannel membrane potential (E_p), but we consider in the next section how E_p would relate to E, depending on structural particulars of a cell junction, and ask whether our results in *Chironomus* are consistent with E_p control of gates.

A model wherein E_p controls gates would simply include these cell-to-cell channels in the realm of other voltage-sensitive channels. As we discuss further on, such a model may extend to amphibian cell-to-cell channels, too.

Perichannel Membrane Potential E_p: Voltage Determinant of Gate Patency?

A priori, one cannot expect that a perichannel membrane potential E_p on a given junction face is necessarily equal to or determined solely by the membrane potential E of the cell to which that face pertains. In a given tissue the perichannel region may be situated deep within a narrow intercellular gap; access to the principal extracellular compartment is thus via a narrow and – in various tissues – more or less long and obstructed pathway. Figure 10 shows a lumped equivalent circuit approximately representing the conductive pathways from the interiors of a coupled cell pair to the extracellular compartment via the intercellular gap. As is shown in Appendix 2, the perichannel membrane potentials E_p for the two sides in the Fig. 10 network may be represented by

$$E_{p1}=E_1-E_g=E_1-k(E_1+E_2)$$
$$E_{p2}=E_2-E_g=E_2-k(E_1+E_2) \qquad (8)$$

where $0<k<\frac{1}{2}$ gives the range of the cross-coefficient k, and where E_g is the potential in the gap at the level of the outer wall of a cell-to-cell channel. In one limiting case ($k=0$), access resistance through the gap (r_g) is negligible in comparison with perichannel membrane resistance (for N channels, r_p/N; *see* Fig. 10), so that $Nr_g/r_p \ll 1$ and

$$E_{p1}=E_1,$$
$$E_{p2}=E_2.$$

In the other limit, access is altogether blocked (for example, by tight junctions), $Nr_g/r_p \gg 1$, and then E_p is specified entirely by, and is proportional to, transjunctional potential E_j:

$$E_{p1}=\frac{E_1-E_2}{2}=\frac{E_j}{2}=-E_{p2}. \qquad (9)$$

(In terms of experimental constraints, *it is important to note that in the latter case perichannel membrane potential E_p on the two junction faces cannot be independently voltage clamped.* Moreover, for one of the two gate populations, $E_p \geqq 0$; and for the other $E_p \leqq 0$.) In the intermediate range of Nr_g/r_p, each side's E_p is influenced by the membrane potentials of both cells, to a degree that depends on r_g.

In many tissues, tight junctions (*zonulae occludentes*) are structural elements that provide high-resistance barriers to diffusion along the gap (e.g., frog skin, Frömter & Diamond, 1972). If such a tight junction, or some other structural element providing an equivalent barrier, were to surround the cell-to-cell channel region of a junction, forming a high perijunctional resistance r_g, then E_p would be determined by E_j alone, and an E_p-dependent g_j would be observed to depend on E_j alone. In *Chironomus,* in contrast to amphibia, g_j is responsive to E rather than to E_j. The limiting case represented by Eq. (9) therefore cannot apply here. Moreover, in intact *Chironomus* salivary gland, tight junctions are absent (Rose, 1971) and there is no reason to expect their formation in cell pairs. If there is any significant resistance in the gap, we consider it would most likely arise along the intermembrane gaps within the cell-to-cell contact regions, and hence would be a distributed resistance.

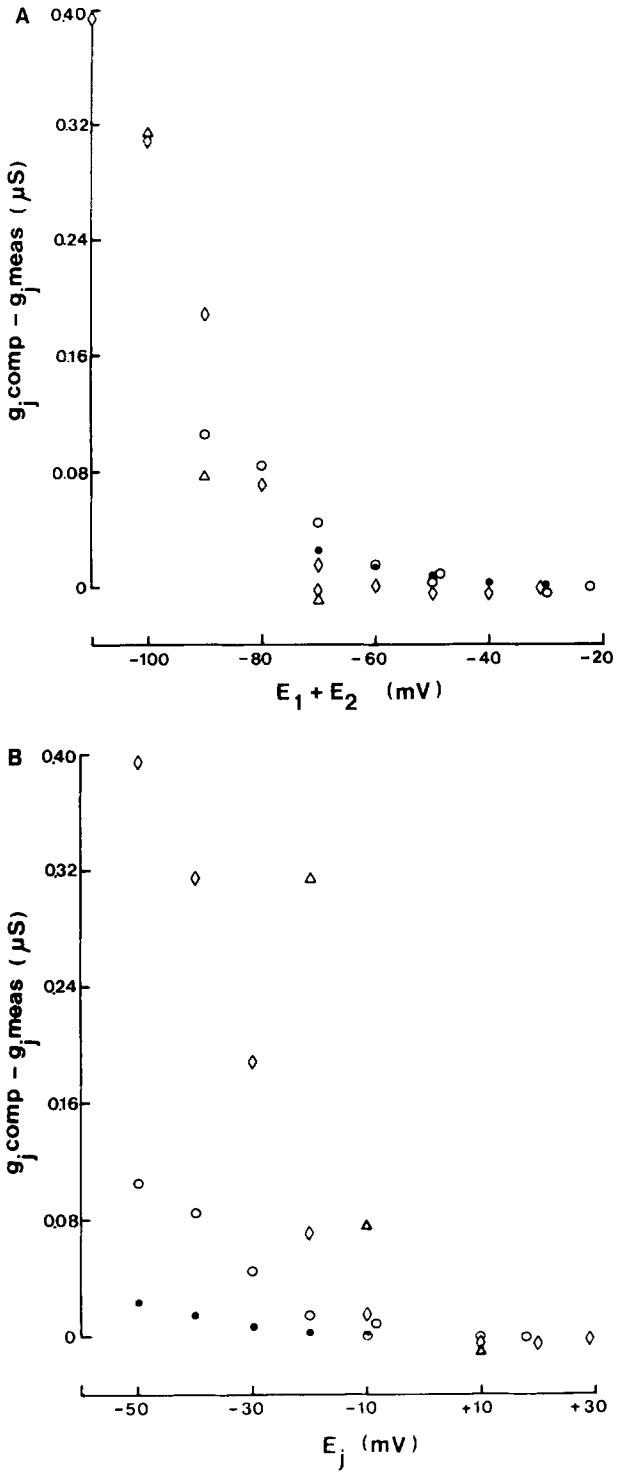

Fig. 11. Comparison of measured and computed g_j when $E_1 \mp E_2$. The experimental information here is taken from Fig. 3*B*. Computed g_j are based on Eq. (3) with $g_j$max, A and E_0 as determined from the data in Fig. 3*B* Inset. The symbols are those used for the corresponding data points in Fig. 3*B*. *(A)*: Ordinates show the deviation of computed from measured g_j values; abscissas are the sums E_1+E_2. *(B)*: The same ordinates as in *A* are plotted against their corresponding E_j. For interpretation, *see* discussion of perichannel membrane potential

If E_p rather than E controls gate patency, and if *Chironomus* junctions have a significant (distributed) r_g – certainly a possibility if we consider the rather extensive and narrow intermembrane gaps separating the cells in a junction – then evidence for gate control by E_p should be sought in g_j measurements made under conditions where E_p is expected to deviate substantially from E. The g_j measured in such a case should differ from that computed from Eq. (3), in which gate patency is considered to be controlled by E. Moreover, the deviation should increase the further E_1+E_2 deviates from zero (Eq. (8)). This test is made in Fig. 11, which plots as ordinates the deviations between the experimental g_j values of Fig. 3*B* and those computed with Eq. (3) for the corresponding E_1, E_2 values. In Fig. 11*A*, the abscissas are the corresponding sums E_1+E_2. The deviation increases as E_1+E_2 increases in magnitude. (If the same ordinates are plotted against their E_j values, as in Fig. 11*B*, the several sets of points for different E_2 values are seen to diverge greatly.) Although the observation that the pattern of g_j deviation follows the expected trend is hardly conclusive evidence, it is consistent with a role for E_p as the determinant of gate patency.

Comparison of the Voltage-Dependent Conductance in Junctions of Chironomus Salivary Gland Cells with that of Amphibian Blastomere Pairs

Studies on cell-to-cell channels in amphibian blastomere pairs indicated that – in striking contrast to our results – the probability of a channel's being open depends, in the steady state, only on the transjunctional potential and not at all on the particular membrane potentials of the joined cells (Spray, Harris & Bennett, 1981*b*). There are some functional as well as structural differences between vertebrate (amphibian) and arthropod (insect) junctions (Epstein & Gilula, 1977; Peracchia, 1973; Flagg-Newton & Loewenstein, 1979; Schwarzmann et al., 1981), but, so far, these provide no compelling reasons to expect fundamental differences in the mechanism of channel patency control. In fact, at least some of the differences in the voltage-dependent g_j properties in the two cases may be less profound than they appear at first – as can be appreciated from the following comparison.

1. Perichannel Membrane Potential Dependence *vs.* Transjunctional Potential Dependence. Phenomenologically, whereas the amphibian channels are

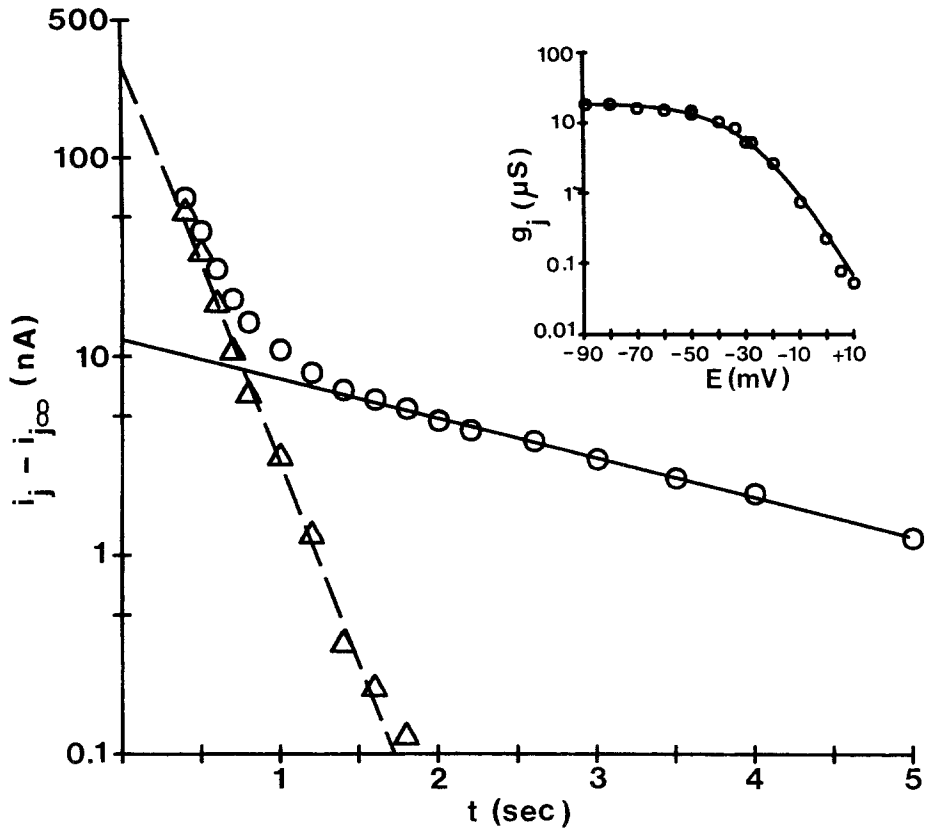

Fig. 12. Kinetics of junctional conductance change following cell depolarization. In this experiment, the potential of cell 2 (E_2) was stepped from an initial potential equal to that of cell 1 ($E_1 = E_2 = -28$ mV) to roughly the antisymmetric potential, +30 mV, while E_1 remained clamped at −28 mV. The kinetics of the ensuing conductance change are represented by the decrease in junctional current i_j ($g_j = i_j/E_j$; and E_j, −58 mV, is constant during the voltage step). The semilogarithmic plot of $i_j - i_{j\infty}$ *vs.* time – where $i_{j\infty} = 7.8$ nA was the steady-state i_j at $E_1 = -28$ mV and $E_2 = +30$ mV – shows two clearly separable time constants: a minor, slow component, $\tau_2 = 2.17$ sec (inverse of slope of solid line, obtained by linear regression of data between $t = 1.6$ and 5 sec; $r = 0.998$; amplitude at $t = 0$: 12 nA), and a major, fast component, $\tau_1 = 0.215$ sec (inverse of slope of dashed line, obtained by linear regression of the difference between data points at $t = 0.4$ sec through $t = 1.6$ sec, and the time-corresponding points on the solid line; $r = 0.998$; amplitude at $t = 0$: 295 nA). (Data for $t < 0.4$ sec were omitted because of the inadequate response time of the recorder for the large initial amplitude of i_j.) The data in Table 1 were also collected from this junction, and the parameters $g_j$max, A and E_0 used in the calculations there were derived from the data shown in the Inset (circles), where the solid line represents Eq. (4), based on those parameters

responsive only to transjunctional potential E_j, the *Chironomus* channels are responsive to membrane potentials. Moreover, in our experiments with $E_1 = -E_2$ the latter channel gates are controlled entirely by E_1 and E_2, and not by E_j. While we suggest that the channel gates in *Chironomus* are controlled by perichannel membrane potential E_p, Harris et al. (1981) have proposed that the amphibian channel gates respond specifically to the transjunctional potential as sensed within the channel. We now examine this apparent difference in channel control in the light of some conclusions from our analysis of E_p: in the limiting case of high diffusion resistance (in the intermembrane gap) between the bath and the channel region of the junction ("perijunctional resistance"), E_p on a junction face becomes equal to $|E_j|/2$, and becomes subject to the constraint $E_{p1} = -E_{p2}$. In that limiting case – which may apply to the amphibian blastomere pair (*see* below) – even if one clamps the two *cells* independently to different potentials, the E_p's are clamped to $\pm E_j/2$, not to E_1, E_2; that is, E_{p1} *and* E_{p2} *then reflect only* E_j. Channel gates that are controlled by E_p then nevertheless *appear* to be controlled by E_j alone; and the consequent steady-state g_j *vs.* E curve assumes the form reported for amphibian blastomere pairs (Spray et al., 1981*b*), peaking at $E_j = 0$, and falling off symmetrically with increasing $|E_j|$.

As already mentioned, tight junctions, the structural elements that commonly serve as high-resistance barriers to diffusion along the gap between cells, are absent in *Chironomus* salivary glands. Amphibian embryo cells, however, do es-

tablish tight junctions during development of the blastocoel (Blueminck, 1970; Selman & Perry, 1970; Kalt, 1971; *see also* Slack & Warner, 1973), and perhaps isolated blastomere pairs, too, develop tight junctions or equivalent barriers that provide a perijunctional resistance. Thus, the possibility remains that in amphibia, too, the cell-to-cell channel gates are controlled by perichannel membrane potential.

2. Voltage-Insensitive Component of g_j. Another phenomenological difference could be explained simply by a perijunctional resistance. In amphibian junctions, Spray et al. (1979, 1981*b*) found that g_j included a voltage-independent component amounting to as much as 5% of their g_j max. No such component was seen in *Chironomus*; in fact, it must have been less than 0.03% of g_j max (Fig. 3*B*, lowest measured g_j value), our limit of resolution. A significant voltage-independent component could arise from a population of potential-insensitive cell-to-cell channels, and this was the interpretation favored by Spray et al. (1981*b*). But alternatively, it would also occur if a junction is surrounded by a high-resistance perijunctional diffusion barrier, so that voltage-insensitive cell membrane channels are included within the appositional region isolated by the barrier.

In sum then, in amphibia, both phenomenologies, the E_j dependence of junctional conductance and the voltage-insensitive component, might be reflections of a perijunctional high-resistance diffusion barrier.

3. Time Course. The time courses of the voltage-dependent junctional conductance changes in *Chironomus* and in amphibia are strikingly similar. The time constants are on the order of tenths of a second in each (Fig. 12 in this report and Harris et al., 1981; *cf. also* Socolar & Politoff, 1971, and Spray et al., 1979). The occurrence of single or double exponential kinetics may depend simply on whether gates change on one or both junction faces (and hence – if the controlling potentials for the two faces differ – with one or two rate constants). In the amphibian studies of Harris et al. (1981), two-exponential kinetics were reported only for experiments in which a sign reversal of E_j was effected. In the experiment of Fig. 12, the primary change in E was that in cell 2. However, if gates are controlled by E_p, the E_2 step could have caused a shift in E_{p1} even though E_1 was held constant. This may account for the minor slow component seen in Fig. 12.

4. Contingent *vs.* Independent Closure of the Two Gates In Series. Perhaps the most distinctive property reported for the amphibian gate is the latter's inability to close in response to an E_j change unless and until the gate in series is open. From this feature – which has no counterpart in our results on *Chironomus* cells, where the gates appear quite independently responsive – it has been argued that the amphibian gate is controlled by the electric field it senses within the channel, a field that is negligible when the gate in series is closed (Harris et al., 1981). This sort of "contingent" behavior would indeed be predicted if the gate's voltage sensor were thought to respond to the electric field within the channel. However, the converse is not compelling. It is possible, for example, to imagine structural (mechanical) constraints that a closed gate might impose on its open partner, preventing the latter's closure as long as the former is closed. Hence it seems premature to conclude that the amphibian channel responds to the transchannel field rather than, say, to the perichannel membrane electric field.

5. Apparent Gating Charge, z. The value of z inferred in the amphibian junction depends on the model chosen for analyzing the experimental data. Harris et al. (1981) give $z = 5.0$–6.3, based on the premise that the voltage-sensing dipole, represented here by the apparent gating charge z, responds to transchannel potential E_j. However, if the gating charge responds to perichannel membrane potential ($E_j/2$ here; Eq. (9)), a model based on transchannel potential (E_j) underestimates A and hence z by a factor 2; thus $z = 10$–12.6 in amphibia if E_p determines g_j. (Since, according to Eq. (A1) in Appendix 1, this doubling would just reflect halving of the relevant membrane thickness M subject to E_j, the change in dipole moment represented by z would be the same for either model.) For *Chironomus* we have derived the value $z \approx 2$. However, this value is underestimated by an undetermined factor if, as our analysis suggests, we are dealing in each junction face with a population of gates that respond to E_p rather than to E. Our assumption of E dependence would thus give rise to an undetermined error in A. This renders meaningless a comparison of z values. It should be noted, nevertheless, that, were z to differ in amphibia and *Chironomus*, this could reflect simply a difference in orientation of dipole moments and need not imply that the moments have dissimilar magnitudes.

In general, the comparison on all five points does not require us at this time to think in terms

of two fundamentally different gating mechanisms for cell-to-cell channels.

We are grateful to J.L. Gray who designed and to E. Smith who built the voltage clamps; to W. Nonner, W.R. Loewenstein, and K.L. Magleby for many helpful discussions, and to A.L. Zimmerman for critical reading of the manuscript. We thank S.I. Brill and A. Cosio for typing the manuscript, and R. Serralta for photography. This investigation was supported by PHS Grant Number 2 R01CA14464, awarded by the National Cancer Institute, DHHS.

Appendix 1

Voltage-Dependent Distribution of Gates Between Open and Closed States; Derivation of Text Equations (2)

The equilibrium distribution of a gate population between open and closed states due to the influence of an electric field is expressible in terms of the Gibbs free energy components for the opening process (*cf.* Ehrenstein, Lecar, & Nossal, 1970; Magleby & Stevens, 1972).

Consider the transition of gates from the closed state X to the open state X^* under the direct or indirect influence of a transmembrane electric field due to membrane potential E. We may interpret the influence of the field to imply that a change of electric dipole moment is associated with gate opening (Magleby & Stevens, 1972; Harris et al., 1981). For example, if the field acts directly on the gates, we assume that in the closed and open states a dipole moment associated with a gate differs in respect to its component parallel to the field. If M represents the membrane thickness across which the potential E is considered to prevail, with a constant field, the field is expressed as E/M. If ϑ is the angle between the inward normal to the cell surface and the dipole, of moment P, then the component of P parallel to the field is $|P|\cos\vartheta$. The transition $X \rightarrow X^*$ is associated with a change in the parallel component of dipole moment from $|P_c|\cos\vartheta_c$ for the closed state to $|P_o|\cos\vartheta_o$ for the open state. The Gibbs free energy per mole of open gates is then

$$G_o = G_o^\circ + RT\ln f_o - \frac{a|EP_o|}{M}\cos\vartheta_o,$$

where a is Avogadro's number, f_o is the fraction of open gates and G_o° is the standard free energy per mole of open gates. The first two terms on the right make up the chemical component of the free energy and the last, the electrical (Debye, 1929; Mayer & Mayer, 1940; the propriety of the negative sign before the electrical term is apparent when we consider that G_o must be lower for a dipole aligned with E ($\cos\vartheta > 0$) than for an antiparallel dipole ($-\cos\vartheta < 0$). Similarly, for closed gates,

$$G_c = G_c^\circ + RT\ln(1-f_o) - \frac{a|EP_c|}{M}\cos\vartheta_c.$$

The free energy change $(G_o - G_c)$ for gate opening is

$$\Delta G = \Delta G^\circ + RT\left(\ln\frac{f_o}{1-f_o}\right) + \frac{a|E|}{M}(|P_c|\cos\vartheta_c - |P_o|\cos\vartheta_o), \tag{A1}$$

where $\Delta G^\circ = G_o^\circ - G_c^\circ$. We note that $(|P_c|\cos\vartheta_c - |P_o|\cos\vartheta_o)$, being the projection of the presumably fixed vector difference $(P_c - P_o)$ onto the field direction, either always has the same sign as E or always has the opposite sign. If we introduce the elementary unit of charge q ($q = F/a$, where F is Faraday's constant), we may then write

$$\Delta G = \Delta G^\circ + RT\left(\ln\frac{f_o}{1-f_o}\right) + zFe \tag{A2}$$

where

$$z = \pm\frac{1}{qM}||P_c|\cos\vartheta_c - |P_o|\cos\vartheta_o|, \tag{A3}$$

and where the positive sign applies if $(|P_c|\cos\vartheta_c - |P_o|\cos\vartheta_o)$ has the same sign as E, the negative sign otherwise (*cf.* Labarca et al., 1980).

It is convenient here to express the electrical component of ΔG as the simpler term zFE, a term we may view as arising in an opening process that is energetically equivalent to the dipole change (although it may be a less realistic model), namely, the transfer of a charge zq inward (i.e., toward the cell interior) across the potential E (Schein, Colombini & Finkelstein, 1976; Ehrenstein & Lecar, 1977). Inasmuch as we find the closed state to be favored at positive E values, we infer that gate opening is associated with inward movement of positive charge – or outward movement of negative charge.

If we consider the open and closed gates to be in equilibrium, we may set $\Delta G = 0$ in Eq. (A2); it follows that the equilibrium fraction of open gates is

$$f_o = \left(1 + \exp\frac{\Delta G^\circ + zFE}{RT}\right)^{-1}$$

which gives text Eq. (2), reflecting a Boltzmann distribution between open and closed states.

We recall that ΔG° is just the molar chemical free energy difference between gates all of which are open and gates all of which are closed. If E_0 is defined as that value of E which, at equilibrium, makes $f_o = \frac{1}{2}$, we may write

$$-\Delta G^\circ = zFE_0 = RTAE_0$$

which defines $A = zF/RT$ (*cf.* Labarca et al., 1980; Harris et al., 1981). It might seem that ΔG° should be a constant for a given kind of cell. However, the empirical finding of considerable variability of E_0 in the present work suggests that the foregoing analysis oversimplifies. (This issue is treated further in the Discussion.) Hence, for the general case, we will admit $\Delta G_1^\circ \neq \Delta G_2^\circ$ for the two gate populations of a junction.

Appendix 2

Perichannel Membrane Potential: Analysis Using a Lumped Resistance Network

The portions of plasma membrane immediately bordering cell-to-cell channels are generally situated deep within a narrow intercellular gap. In particular cell types, these membrane portions may be isolated from the main extracellular compartment (that bathes the great majority of the cell's plasma membrane) by considerable electrical resistance – i.e., by a diffusion barrier. In such cases, the potential across an element of perichannel membrane on one cell face of the junction is influenced by the membrane potential of the partner cell and therefore cannot simply equal the nonjunctional membrane potential of the first cell.

To illustrate the range of possible effects on perichannel membrane potential, including the limiting case of very high gap resistance, we analyze a lumped equivalent circuit that approximately represents the conductive pathways from the interiors of a coupled cell pair to the bathing medium outside

(Fig. 10). In the perichannel membrane element r_p shown on side 1, the outward current is $(E_1 - E_g)/r_p$; and, on side 2, $(E_2 - E_g)/r_p$. If the junction comprises N channels and N such pairs of perichannel membrane elements, the combined outward current is $N(E_1 + E_2 - 2E_g)/r_p$. Since this same current flows across the gap resistance r_g to ground,

$$\frac{N(E_1 + E_2 - 2E_g)}{r_p} = \frac{E_g}{r_g}.$$

Hence

$$E_g = \frac{Nr_g(E_1 + E_2)}{r_p + 2Nr_g}$$

and the perichannel membrane potential of the element on side 1 is

$$E_1 - E_g = \frac{(r_g + Nr_g)E_1 - Nr_g E_2}{r_p + 2Nr_g}.$$

This can be represented simply as

$$E_1 - E_g = (1 - k)E_1 - kE_2$$

where the cross-coefficient $k = Nr_g/(r_p + 2Nr_g)$, so that depending on the ratio Nr_g/r_p we have a range of k variation, $0 < k < \frac{1}{2}$.

A quite similar result is obtained from a calculation that assumes (1) a continuous distribution of perichannel membrane (and, hence, of current sources) along planar cell faces bounding a junctional gap; (2) distributed resistance of the electrolyte in the gap; and (3) a lumped r_g component (localized barrier) within the gap.

References

Blueminck, J.G. 1970. The first cleavage of the amphibian egg. An electron microscope study of the onset of cytokinesis in the egg of *Amblystoma mexicanum*. *J. Ultrastruct. Res.* **32**:142–166

Dahl, G., Isenberg, G. 1980. Decoupling of heart muscle cells: Correlation with increased cytoplasmic calcium activity and with changes of nexus ultrastructure. *J. Membrane Biol.* **53**:63–75

Debye, P. 1929. Polar Molecules. Dover, New York

Délèze, J. 1970. The recovery of resting potential and input resistance in sheep heart injured by knife or laser. *J. Physiol. (London)* **208**:547–564

Ehrenstein, G., Lecar, H. 1977. Electrically gated ionic channels in lipid bilayers. *Q. Rev. Biophys.* **10**:1–34

Ehrenstein, G., Lecar, H., Nossal, R. 1970. The nature of the negative resistance in bimolecular lipid membranes containing excitability-inducing material. *J. Gen. Physiol.* **55**:119–133

Epstein, M.L., Gilula, N.B. 1977. A study of communication specificity between cells in culture. *J. Cell Biol.* **75**:769–787

Flagg-Newton, J., Loewenstein, W.R. 1979. Experimental depression of junctional membrane permeability in mammalian cell culture: A study with tracer molecules in the 300 to 800 dalton range. *J. Membrane Biol.* **50**:65–100

Frömter, E., Diamond, J. 1972. Route of passive ion permeation in epithelia. *Nature (London)* **235**:9–13

Harris, A.L., Spray, D.C., Bennett, M.V.L. 1981. Kinetic properties of a voltage-dependent junctional conductance. *J. Gen. Physiol.* **77**:95–117

Johnston, M.F., Ramon, F. 1981. Electrotonic coupling in internally perfused crayfish segmented axons. *J. Physiol. (London)* **317**:509–518

Kalt, M.R. 1971. The relationship between cleavage and blastocoel formation in *Xenopus laevis*. II. Electron microscope observations. *J. Embryol. Exp. Morphol.* **26**:51–66

Labarca, P., Coronado, R., Miller, C. 1980. Thermodynamic and kinetic studies of the gating behavior of a K^+-selective channel from the sarcoplasmic reticulum membrane. *J. Gen. Physiol.* **76**:397–424

Loewenstein, W.R. 1966. Permeability of membrane junctions. *Ann. N.Y. Acad. Sci.* **137**:441–472

Loewenstein, W.R. 1981. Junctional intercellular communication: The cell-to-cell membrane channel. *Physiol. Rev.* **61**:829–913

Loewenstein, W.R., Nakas, M., Socolar, S.J. 1967. Junctional membrane uncoupling. Permeability transformation at a cell membrane junction. *J. Gen. Physiol.* **50**:1865–1891

Loewenstein, W.R., Rose, B. 1979. Calcium in (junctional) intercellular communication and a thought on its behavior in intracellular communication. *Ann. N.Y. Acad. Sci.* **307**:285–307

Magleby, K., Stevens, C.F. 1972. A quantitative description of endplate currents. *J. Physiol. (London)* **223**:173–197

Mayer, J.E., Mayer, M.G. 1940. Statistical Mechanics. John Wiley & Sons, New York

Obaid, A.L., Rose, B. 1981*a*. Junctional resistance of *Chironomus* cell pairs depends on (nonjunctional) membrane potential. *Biophys. J.* **33**:106*a*

Obaid, A.L., Rose, B. 1981*b*. Modulation of cell junction conductance by membrane potential. *Abstr.* VII *Intl. Biophys. Congr.*, 154

Oliveira-Castro, G.M., Loewenstein, W.R. 1971. Junctional membrane permeability: Effects of divalent cations. *J. Membrane Biol.* **5**:51–77

Peracchia, C. 1973. Low resistance junctions in crayfish. II. Structural details and further evidence for intercellular channels by freeze fracture and negative staining. *J. Cell Biol.* **57**:66–80

Politoff, A.L., Socolar, S.J., Straus, S.E. 1970. Electrically-elicited uncoupling of a low resistance cell junction. *Biophys. J.* **10**:75*a*

Rose, B. 1970. Junctional membrane permeability: Restoration by repolarizing current. *Science* **169**:607–609

Rose, B. 1971. Intercellular communication and some structural aspects of membrane junctions in a simple cell system. *J. Membrane Biol.* **5**:1–19

Rose, B., Loewenstein, W.R. 1971. Junctional membrane permeability. Depression by substitution of Li for extracellular Na, and by long-term lack of Ca and Mg.; restoration by cell repolarization. *J. Membrane Biol.* **5**:20–50

Rose, B., Loewenstein, W.R. 1976. Permeability of a cell junction and the local cytoplasmic free ionized calcium concentration: A study with aequorin. *J. Membrane Biol.* **28**:87–119

Rose, B., Rick, R. 1978. Intracellular pH, intracellular free Ca, and junctional cell-cell coupling. *J. Membrane Biol.* **44**:377–415

Schein, S.J., Colombini, M., Finkelstein, A. 1976. Reconstitution in planar lipid bilayers of a voltage-dependent anion-selective channel obtained from Paramecium mitochondria. *J. Membrane Biol.* **30**:99–120

Schwarzmann, G., Wiegandt, H., Rose, B., Zimmerman, A.L., Ben-Haim, D., Loewenstein, W.R. 1981. Diameter of the cell-to-cell junctional channels as probed with neutral molecules. *Science* **213**:551–553

Selman, G.J., Perry, M.M. 1970. Ultrastructural changes in the surface layers of the newt's egg in relation to the mechanism of its cleavage. *J. Cell Sci.* **6**:207–229

Slack, C., Warner, A.E. 1973. Intracellular and intercellular

potentials in the early amphibian embryo. *J. Physiol. (London)* **232**:313–330

Socolar, S.J. 1977. Appendix: The coupling coefficient as an index of junctional conductance. *J. Membrane Biol.* **34**:29–37

Socolar, S.J., Politoff, A.L. 1971. Uncoupling cell junctions of a glandular epithelium by depolarizing current. *Science* **172**:492–494

Spray, D.C., Harris, A.L., Bennett, M.V.L. 1979. Voltage dependence of junctional conductance in early amphibian embryos. *Science* **204**:432–434

Spray, C.D., Harris, A.L., Bennett, M.V.L. 1981*a*. Gap junctional conductance is a simple and sensitive function of intracellular pH. *Science* **211**:712–715

Spray, C.D., Harris, A.L., Bennett, M.V.L. 1981*b*. Equilibrium properties of a voltage dependent junctional conductance. *J. Gen. Physiol.* **77**:77–93

Spray, D.C., Harris, A.L., Bennett, M.V.L. 1982*a*. Comparison of pH and calcium dependence of gap junctional conductance. *In:* Intracellular pH. Its measurement, regulation and utilization in cellular functions. R. Nuccitelli and D.W. Deamer, editors. Kroc Foundation Series Vol. 15, pp. 445–458. Alan R. Liss, New York

Spray, D.C., Stern, J.H., Harris, A.L., Bennett, M.V.L. 1982*b*. Gap junctional conductance: Comparison of sensitivities to H and Ca ions. *Proc. Natl. Acad. Sci. USA* **79**:441–445

Thomas, R.C. 1974. Intracellular pH of snail neurones measured with a new pH-sensitive glass micro-electrode. *J. Physiol. (London)* **238**:159–180

Turin, L., Warner, A.E. 1977. Carbon dioxide reversibly abolishes ionic communication between cells of early amphibian embryos. *Nature (London)* **270**:56–57

Turin, L., Warner, A.E. 1980. Intracellular pH in early *Xenopus* embryos: Its effect on current flow between blastomeres. *J. Physiol. (London)* **300**:489–504

Received 19 July 1982; revised 17 November 1982

Note Added in Proof

Since submission of our manuscript, Johnston and Ramon (*Biophys. J.* **39**:115–117 (1982)) have reported that g_j of the electrical synapse of the crayfish is voltage insensitive. In their experiments, the axons on both sides of the synapse were perfused; it is not known whether the synapse between unperfused axons also is voltage insensitive.